

Prediction models for network-linked data

Tianxi Li, Elizaveta Levina, Ji Zhu

Department of Statistics,
University of Michigan, Ann Arbor

December 3, 2024

Abstract

Prediction problems typically assume the training data are independent samples, but in many modern applications samples come from individuals connected by a network. For example, in adolescent health studies of risk-taking behaviors, information on the subjects' social networks is often available and plays an important role through network cohesion, the empirically observed phenomenon of friends behaving similarly. Taking cohesion into account in prediction models should allow us to improve their performance. Here we propose a regression model with a network-based penalty on individual node effects to encourage similarity between predictions for linked nodes, and show that it performs better than traditional models both theoretically and empirically when network cohesion is present. The framework is easily extended to other models, such as the generalized linear model and Cox's proportional hazard model. Applications to predicting levels of recreational activity and marijuana usage among teenagers based on both demographic covariates and their friendship networks are discussed in detail and demonstrate the effectiveness of our approach.

1 Introduction

Advances in data collection and social media have resulted in network data being collected in many applications, recording relational information between units of analysis; for example, information about friendships between adolescents is now frequently available in studies of health-related behaviors [40, 43, 44, 14]. This information is often collected along with more traditional covariates on each unit of analysis; in the adolescent example, these may include variables such as age, gender, race, socio-economic status, academic achievement, etc. There is a large body of work extending over decades on predicting a response variable of interest from such covariates, via linear or generalized linear models, survival analysis, classification methods, and the like, which typically assume the training samples are independent and do not extend to situations where the samples are connected by a network. There is also now a large body of work focusing on analyzing the network structure implied by the relational data alone, for example, detecting communities; see [20, 22] for reviews. The more traditional covariates, if used at all in such network analyses, are typically used to help analyze the network itself, e.g., find better communities [7, 41, 69]. There has not been much focus on developing a general statistical framework for using network data in prediction, although there are methods available for specific applications [66, 2, 60].

In the social sciences and especially in economics, on the other hand, there has been a lot of recent interest in causal inference on the relationship between a response variable and both covariates and network influences [51, 39]. While in certain experimental settings such inference is possible [47, 13, 45], in most observational studies on networks establishing causality is substantially more difficult than in regular observational studies. While network cohesion (a generic term by which in this paper we mean linked nodes acting similarly) is a well known phenomenon observed in numerous social behavior studies [21, 24], explaining it causally on the basis of observational data is very challenging. An excellent analysis of this problem can be found in [51], showing that it is in general impossible to distinguish network cohesion resulting from homophily (nodes become connected because they act similarly) and cohesion resulting from contagion (behavior spreads from node to node through the links), and to separate that from the effect of node covariates themselves. However, making good predictions of node behavior is an easier task than causal inference, and is often all we need for practical purposes. Our goal in this paper is to take advantage of the network cohesion phenomenon in order to better predict a response variable associated with the network nodes, using both node covariates and network information. While we do not attempt to make causal inferences, we focus on interpretable models where effects of individual variables can be explicitly estimated.

Using network information in predictive models has not yet been well studied. Most classical predictive models treat the training data as independently sampled from one common population, and, unless explicitly modeled, network cohesion violates virtually all assumptions that provide performance guarantees. More importantly, cohesion is potentially helpful in making predictions, since it suggests pooling information from neighboring nodes. In certain specific contexts, regression with dependent observations has been studied. For example, in econometrics, following the concepts initially discussed in [38], assuming some type of an auto-regressive model on the response variables is common, such as the basic autoregressive model in [10] and its variants including group interactions and group fixed effects [32]. Such models assume specific forms of different types of network effects, namely, endogenous effects, exogenous effects and correlated effects, and most of this literature is focused on identifiability of such effects. In [10, 36], these ideas were applied to the adolescent health data from the AddHealth study [23] which we discuss in detail in Section 5. However, these methods have mainly been used to identify social effects in a very specific format, without a focus on interpretability or good prediction performance. For instance, including neighbors' responses as covariates in linear regression makes interpretation of other covariate effects more difficult. In addition, they do not extend easily beyond linear regression (for example, to generalized linear models and Cox's proportional hazard model).

Our approach is to introduce network cohesion into regression using the idea of fusion penalties [30, 57], framing the problem as penalized regression. Fusion penalties based on a network have been used in variable selection [33, 34, 42, 26], but this line of work is not directly relevant here since we are interested in using the network of observations, not variables. However, our approach can be viewed as a regression version of the point estimation problem discussed in [52, 64]. We show that our method gives consistent estimates of covariate effects and can be directly extended to generalized linear models and survival analysis; we also derive explicit conditions on when enforcing network cohesion in regression can be expected to perform better than ordinary least squares. In contrast to previous work, we assume no specific form for the cohesion effects and require no information about potential groups. We also derive a computationally efficient algorithm for implementing our approach, which is efficient for both sparse and dense networks, the latter with an extra sparsification step which we prove preserves the relevant network properties. To the best

of our knowledge, this is the first proposal of a general regression framework with network cohesion among the observations that is computationally feasible and can retain covariate interpretations as well as make out-of-sample predictions.

The rest of this paper is organized as follows. In Section 2, we introduce our approach in the setting of linear regression as a penalized least squares problem and demonstrate its Bayesian interpretation and the connection to linear mixed effects models. The idea is then extended to generalized linear models. Finite-sample and asymptotic properties are discussed in Section 3. Simulation results demonstrating the theoretical bounds and the advantage over regression without using networks are presented in Section 4. Section 5 discusses two examples in detail, applying our method to predict levels of recreational activity and marijuana usage among teenagers.

The algorithms in this paper are implemented in the R package **netcoh** [35], available on CRAN. Code for the examples in the paper can be found on the authors’ webpage.

2 Regression with network cohesion

2.1 Set-up and notation

We start from setting up notation. By default, all vectors are treated as column vectors. The data consist of n observations $(y_1, \mathbf{x}_1), (y_2, \mathbf{x}_2), \dots, (y_n, \mathbf{x}_n)$, where $y_i \in \mathbb{R}$ is the response variable and $\mathbf{x}_i \in \mathbb{R}^p$ is the vector of covariates for observation i . We write $\mathbf{Y} = (y_1, y_2, \dots, y_n)^T$ for the response vector, and $\mathbf{X} = (\mathbf{x}_1, \mathbf{x}_2, \dots, \mathbf{x}_n)^T$ for the $n \times p$ design matrix. We treat \mathbf{X} as fixed and assume its columns have been standardized to have mean 0 and variance 1. We also observe the network connecting the observations, $\mathcal{G} = (V, E)$, where $V = \{1, 2, \dots, n\}$ is the node set of the graph, and $E \subset V \times V$ is the edge set. We represent the graph by its adjacency matrix $A \in \mathbb{R}^{n \times n}$, where $A_{uv} = 1$ if $(u, v) \in E$ and 0 otherwise. We assume there are no loops so $A_{vv} = 0$ for all $v \in V$, and the network is undirected, i.e., $A_{uv} = A_{vu}$. The (unnormalized) Laplacian of \mathcal{G} is given by $L = D - A$, where $D = \text{diag}(d_1, d_2, \dots, d_n)$ is the degree matrix, with node degree d_u defined by $d_u = \sum_{v \in V} A_{uv}$.

2.2 Linear regression with network cohesion

We start from discussing what we mean by the term “cohesion”. This is a vague term which can be interpreted in several ways depending on whether it refers to the network itself or both the network and additional covariates. Cohesion defined on the network alone can be reflected in various properties, such as local density, connectivity and community structure; we refer the readers to Chapter 4 of [27] for details. In the context of regression on networks which is the focus of this paper, two types of cohesion are commonly discussed: homophily (also known as assortative mixing) and contagion. Homophily means nodes similar in their characteristics tend to connect, with the implication of a causal direction from sharing individual characteristics to forming a connection. In contrast, contagion means that nodes tend to behave similarly to their neighbors, with a causal direction from having a connection to exhibiting similar characteristics. Distinguishing these two phenomena in an observational study without additional strong assumptions is not possible [51]. Nonetheless, both of these indicate a correlation between network connections and node similarities, observed

empirically by many social behavior studies [24, 44, 21], and that is all we need and assume in this paper. We use the generic term “cohesion” in order to cover both possibilities of homophily and contagion, which we do not need to distinguish.

While the regularization idea for encouraging network cohesion is general, it is simplest to demonstrate in the context of linear regression, so we start from this setting. Assume that

$$\mathbf{Y} = \boldsymbol{\alpha} + X\boldsymbol{\beta} + \boldsymbol{\epsilon} \quad (1)$$

where $\boldsymbol{\alpha} = (\alpha_1, \alpha_2, \dots, \alpha_n)^T \in \mathbb{R}^n$ is the vector of individual node effects, and $\boldsymbol{\beta} = (\beta_1, \beta_2, \dots, \beta_p)^T \in \mathbb{R}^p$ is the vector of regression coefficients. At this stage, no assumption on the distribution of the error $\boldsymbol{\epsilon}$ is needed, but we assume $\mathbb{E}\boldsymbol{\epsilon} = \mathbf{0}$ and $\text{Var}(\boldsymbol{\epsilon}) = \sigma^2 I_n$, where I_n is the $n \times n$ identity matrix. For simplicity, we further assume that $n > p$ and $X^T X$ is invertible. If $p > n$ and this is not the case, the usual remedies such as a lasso penalty on $\boldsymbol{\beta}$ can be applied; our focus here, however, is on regularizing the individual effects, and so we will not focus on additional regularization on $\boldsymbol{\beta}$ that may be necessary.

Including the individual node effects $\boldsymbol{\alpha}$ instead of a common shared intercept turns out to be key to incorporating network cohesion. In general $\boldsymbol{\alpha}$ and $\boldsymbol{\beta}$, which add up to $n + p$ unknown parameters, cannot be estimated from the n observations without additional assumptions. One well-known example of such assumptions is the simple fixed effects model (see e.g. [50]), when n samples come from known groups, and within each group individuals share a common intercept. Here, we regularize the problem through a network cohesion penalty on $\boldsymbol{\alpha}$ instead of making explicit assumptions about any structure in $\boldsymbol{\alpha}$.

The regression with network cohesion (RNC) estimator we propose is defined as the minimizer of the objective function

$$L(\boldsymbol{\alpha}, \boldsymbol{\beta}) = \|\mathbf{Y} - X\boldsymbol{\beta} - \boldsymbol{\alpha}\|^2 + \lambda \boldsymbol{\alpha}^T L \boldsymbol{\alpha}, \quad (2)$$

where $\|\cdot\|$ is the L_2 vector norm and $\lambda > 0$ is a tuning parameter. An equivalent and more intuitive form of the penalty, which follows from a simple property of the graph Laplacian, is

$$\boldsymbol{\alpha}^T L \boldsymbol{\alpha} = \sum_{(u,v) \in E} (\alpha_u - \alpha_v)^2. \quad (3)$$

Thus, we penalize differences between individual effects of nodes connected by an edge in the network. We call this term the *cohesion penalty* on $\boldsymbol{\alpha}$. We assume that the effect of covariates X is the same across the network; as with any linear regression, two nodes with similar covariates will have similar values of $\mathbf{x}^T \boldsymbol{\beta}$, and the cohesion penalty makes sure the neighboring nodes have similar individual effects α . Note that this is different from imposing network homophily (which would require nodes with similar covariates to be more likely to be connected).

A path of work in statistics that involves the cohesion penalty is from the variable selection methods of [33, 34], where a network is given between the predictors and as standard regression model is assumed for all individuals. Notice our problem is totally different in that we are considering varying models across observations so the penalty is introduced on the n different individuals. Moreover, though assuming similar covariate effects for connected covariates as in [33] may be helpful in certain problems, it is not clear how widely such assumption holds in general applications. On the other hand, socially connected individuals have similar properties have been widely observed in a wide range of studies [40, 43, 44, 14]. The cohesion penalty is also used in many semi-supervised learning problems and we will

discuss the connections in Section 2.5.

The minimizer of (2) can be computed explicitly (if it exists) as

$$\hat{\boldsymbol{\theta}} = (\hat{\boldsymbol{\alpha}}, \hat{\boldsymbol{\beta}}) = (\tilde{X}^T \tilde{X} + \lambda M)^{-1} \tilde{X}^T \mathbf{Y}. \quad (4)$$

Here, $\tilde{X} = (I_n, X)$ and

$$M = \begin{bmatrix} L & 0_{n \times p} \\ 0_{p \times n} & 0_{p \times p} \end{bmatrix}$$

where $0_{a \times b}$ is an $a \times b$ matrix of all zeros. The estimator exists if $\tilde{X}^T \tilde{X} + \lambda M$ is invertible. Note that

$$\tilde{X}^T \tilde{X} + \lambda M = \begin{bmatrix} I_n + \lambda L & X \\ X^T & X^T X \end{bmatrix}, \quad (5)$$

so it is positive definite if and only if the Schur complement $I_n + \lambda L - X(X^T X)^{-1} X^T = P_{X^\perp} + \lambda L$ is positive definite. From (3), we can see that L is positive semi-definite but singular since $L\mathbf{1}_n = 0$ where $\mathbf{1}$ is the vector of all ones, and thus in principle the estimator may not be computable. In Section 3, we will give an interpretable theoretical condition for the estimator to exist. In practice, a natural solution is to ensure numerical stability by replacing L with the regularized Laplacian $L + \gamma I$, where γ is a small positive constant. Then the estimator always exists, and in fact the regularized Laplacian may better represent certain network properties, as discussed by [12, 1, 31] and others. The resulting penalty is

$$\sum_{(u,v) \in E} (\alpha_u - \alpha_v)^2 + \gamma \sum_v \alpha_v^2, \quad (6)$$

which one can also interpret as adding a small ridge penalty on α for numerical stability.

The penalty (6) suggests a natural baseline comparison to our model which can be used to assess whether cohesion is in fact present in the data. If the graph has no edges (i.e., no information about network connections can be used), the penalty (with $\gamma = 1$) reduces to a ridge penalty on the individual effects α . The regression estimate is minimizing

$$L_n(\boldsymbol{\alpha}, \boldsymbol{\beta}) = \|\mathbf{Y} - X\boldsymbol{\beta} - \boldsymbol{\alpha}\|^2 + \lambda \|\boldsymbol{\alpha}\|^2, \quad (7)$$

We call this *null* model as comparing the prediction error of this model to that of RNC provides qualitative evidence of cohesion. In the case of linear regression, it can be shown that the null model gives exactly the same estimate of $\boldsymbol{\beta}$ as OLS (Lemma 3 in appendix).

Remark 1. The fixed effects regression model with subjects divided into groups can be viewed as a special case of RNC. If the graph \mathcal{G} represents the groups as cliques (everyone within the same group is connected), there are no connections between groups, and we let $\lambda \rightarrow \infty$, then all nodes in one group will share a common intercept.

2.3 Network cohesion for generalized linear models and Cox's proportional hazard model

The RNC methodology extends naturally to generalized linear models and many other regression or classification models such as Cox's proportional hazard model [17] for survival problems and support vector machines [58] for classification using the formulation of [62]. For any generalized linear model with a link function $\phi(\mathbb{E}\mathbf{Y}) = X\boldsymbol{\beta} + \boldsymbol{\alpha}$, where $\boldsymbol{\alpha} \in \mathbb{R}^n$

are the individual effects, suppose the log-likelihood (or partial log-likelihood) function is $\ell(\boldsymbol{\alpha}, \boldsymbol{\beta}; X, \mathbf{Y})$. Then if the observations are linked by a network, to induce network cohesion one can fit the model by maximizing the penalized likelihood

$$\ell(\boldsymbol{\alpha} + X\boldsymbol{\beta}; \mathbf{Y}) - \lambda \boldsymbol{\alpha}^T (L + \gamma I) \boldsymbol{\alpha}. \quad (8)$$

When ℓ is concave in $\boldsymbol{\alpha}$ and $\boldsymbol{\beta}$, which is the case for exponential families, the optimization problem can be solved via Newton-Raphson or another appropriate convex optimization algorithm. Note that the quadratic approximation to (8) is the quadratic approximation to the log-likelihood plus the penalty, and thus the problem can be efficiently solved by iteratively reweighted linear regression with network cohesion, just like the GLM is fitted by iteratively reweighted least squares. The ridge penalty term γI helps with numerical stability and avoids fitted probabilities of 0 and 1 for isolated nodes, which may cause the iterative algorithm to diverge; as discussed in the previous section, adding this term to the Laplacian also improves its representation of the underlying network structure.

RNC can be similarly generalized to Cox's proportional hazard model [17]. In this setting, we observe times until some event occurs, called survival times, which may be censored (unobserved) if the event has not occurred for a particular node. Cox's model assumes the hazard function $h_v(y)$ for each individual v is

$$h_v(y) = h_0(y) \exp(\mathbf{x}_v^T \boldsymbol{\beta}), v \in V,$$

where y is the survival time, \mathbf{x}_v is the vector of p observed covariates for individual v , $\boldsymbol{\beta} \in \mathbb{R}^p$ is the coefficient vector and h_0 is an unspecified baseline hazard function. When we have observations connected by a network, as in the RNC setting, we can also model the individual effects and then encourage network cohesion. Thus we will assume the hazard for each node v is given by

$$h_v(y) = h_0(y) \exp(\mathbf{x}_v^T \boldsymbol{\beta} + \alpha_v), v \in V, \quad (9)$$

where α_v is the individual effect of node v . The appropriate loss function in terms of the parameters $\boldsymbol{\theta} = (\boldsymbol{\alpha}, \boldsymbol{\beta})$ is the partial log-likelihood

$$\ell(\boldsymbol{\theta}; \mathbf{y}) = \sum_v \delta_v \left[\mathbf{x}_v^T \boldsymbol{\beta} + \alpha_v - \log \left(\sum_{u: y_u \geq y_v} \exp(\mathbf{x}_u^T \boldsymbol{\beta} + \alpha_u) \right) \right] \quad (10)$$

where y_v is the observed survival time for node v , and δ_v is the censoring indicator, which is 0 if the observation is right-censored and 1 otherwise. Note that the partial log-likelihood is invariant under a shift in $\boldsymbol{\alpha}$ since such a shift can always be absorbed into h_0 . Thus for identifiability, we require $\sum \alpha_v = 0$. For fixed covariates \mathbf{x}_v , α_v is the individual deviation from the population average log hazard. The sum-to-zero constraint can be automatically enforced by replacing the network Laplacian L in the network cohesion penalty with its regularized version $L + \gamma I$, or equivalently adding a ridge penalty on α 's. Thus we maximize the following objective function, adding a regularized cohesion penalty to the partial log-likelihood:

$$\ell(\boldsymbol{\theta}) - \lambda \boldsymbol{\alpha}^T (L + \gamma I) \boldsymbol{\alpha}.$$

2.4 A Bayesian interpretation

The RNC estimator can also be derived from a Bayesian regression model. Consider the model

$$\mathbf{Y}|\boldsymbol{\alpha}, \boldsymbol{\beta} \sim \mathcal{N}(\boldsymbol{\alpha} + \mathbf{X}\boldsymbol{\beta}, \sigma^2 \mathbf{I}), \quad \boldsymbol{\beta} \sim \pi_{\boldsymbol{\beta}}(\boldsymbol{\phi}), \quad \boldsymbol{\alpha} \sim \pi_{\boldsymbol{\alpha}}(\Phi),$$

where $\pi_{\boldsymbol{\beta}}(\boldsymbol{\phi})$ is the prior for $\boldsymbol{\beta}$ with hyperparameter $\boldsymbol{\phi}$, $\pi_{\boldsymbol{\alpha}}(\Phi)$ is the prior for $\boldsymbol{\alpha}$ with hyperparameter Φ , and σ^2 is assumed to be known. Suppose we take $\pi_{\boldsymbol{\beta}}(\boldsymbol{\phi})$ to be the non-informative Jeffrey's prior, reflecting lack of prior knowledge about the coefficients, and set $\pi_{\boldsymbol{\beta}}(\boldsymbol{\phi}) \propto 1$. For $\boldsymbol{\alpha}$, assume a Gaussian Markov random field (GMRF) prior $\pi_{\boldsymbol{\alpha}} = \mathcal{N}_{\mathcal{G}}(\mathbf{0}, \Phi)$, where $\Phi = \Omega^{-1} = \zeta^2(L + \gamma I)^{-1}$. Note that when $\gamma = 0$, Ω is not invertible, and $\pi_{\boldsymbol{\alpha}}$ is an improper prior called intrinsic GMRF [48].

If the posterior modes are used as the estimators for $\boldsymbol{\alpha}$ and $\boldsymbol{\beta}$, then this is equivalent to (2) with $\lambda = \sigma^2/\zeta^2$ and the Laplacian replaced by the regularized Laplacian $L + \gamma I$. Thus the estimator of (2) is the Bayes estimator with the improper intrinsic GMRF prior over the network on $\boldsymbol{\alpha}$. Note that this Bayesian interpretation is also valid for the generalized linear models.

2.5 Connection to other models

Mixed effects models This connection is directly available from our discussion of the Bayesian interpretation. If we think of $\boldsymbol{\alpha}$ as random effects in a mixed model, then instead of repeated measurements we can view the Bayesian interpretation of our method as inducing correlations between the random effects, $\boldsymbol{\alpha} \sim \mathcal{N}_{\mathcal{G}}(\mathbf{0}, \Phi)$. The estimator (4) is then the mixed model equation in [25] for estimating fixed effects and predicting random effects simultaneously (see [50]). However, the framework of mixed models requires stronger assumptions as it assumes specific format of the variance components. Moreover, (generalized) mixed models are not designed for predictions conceptually. As we will show in our simulation study, the null model (which can be seen as a more standard mixed effects model) is clearly inferior in out-of-sample predictions.

Spatial prediction In spatial problems, data points are typically indexed by their locations. Then a neighborhood weight matrix A can be computed as a function of some distance between locations, and A can be viewed as a weighted analogue of our network adjacency matrix. This leads to natural connections between RNC and methods used in spatial statistics. In particular, ignoring the covariates X , RNC reduces to the Laplacian smoothing point estimation procedure in [52, 64], which is equivalent to Kriging in spatial statistics [18]. [67] shows that a wide class of semi-supervised learning methods based on Laplacian smoothing has interpretations as a graph Kriging. From this perspective, RNC can be seen as a generalization of the graph Kriging of [67] to incorporate covariates and general loss functions. Actually, with covariates X included, the Bayesian interpretation of RNC assumes the same Gaussian Markov random field distribution for $\boldsymbol{\alpha}$ as the one assumed for spatial errors in the conditional autoregressive model (CAR) [6] in spatial regression and its GLM generalization (Chapter 9 of [63]). However, ζ^2 and σ^2 in our Bayesian interpretation are treated as parameters in the CAR, while $\lambda = \sigma^2/\zeta^2$ is treated as a tuning parameter in RNC. Further, the CAR model is fitted either by maximum likelihood involving computationally expensive integration steps, or by posterior inference via Markov chain Monte

Carlo after assuming a full Bayesian model (with additional priors on β and ζ^2 , etc). Both ways involve much heavier computations than RNC, especially for GLM where the Gaussian Markov random field is no longer a conjugate prior. More importantly, CAR models cannot be applied to general loss functions that are not a well-defined likelihood function as in the case of Cox’s model and SVM. Also, CAR models suffer from conceptual difficulties in making out-of-sample predictions [63]. In contrast, RNC provides a universal strategy under general loss functions and comes with a natural out-of-sample predictor, discussed in Section 2.6.

Manifold embeddings Our Laplacian-based penalty has connections to the substantial literature on manifold embeddings and semi-supervised learning. The general idea there is to embed data points which is usually in high dimension Euclidean space equipped with some non-Euclidean similarity measure (e.g., an adjacency matrix) into Euclidean space, and then use the Euclidean coordinates of the data points for the task at hand, for example clustering [53] or visualization [56]. In comparison, we assume the network is given instead of constructed from some original features. Perhaps the algorithm most closely related to ours is Laplacian Eigenmaps [3], which proposed using k eigenvectors of the constructed graph Laplacian L corresponding to the smallest eigenvalues as the Euclidean embedding of the graph in order to obtain a low-dimensional representation of the data. The early manifold literature focused on the unsupervised task of embedding the given data and cannot be generalized to new data. Semi-supervised learning problems instead assume that predictors are observed but only part of the labels are given. With the network constructed from predictors, training can be done and predictions can be made on the unobserved labels by the idea of Eigenmaps [70]. The idea is then extended to directed graphs [71]. In these methods, prediction task is not for new samples as in our setting, since essentially the network structure between training data and test data is assumed to be known. However, later extensions [5, 11, 61] were developed by assuming the embedding coordinates take certain specific forms as functions of the original data points, enabling out-of-sample embedding after estimating the functions. A more relevant work is from [4] in which the estimation procedure is formed under the regularization framework. However, all the above literature assume the input features are given in Euclidean space, for which smoothness well defined and and functional embedding is naturally available after functional estimation. When the network alone is given without the original data points available in the context of multivariate analysis, there are no out-of-sample extensions that we are aware of. In contrast, our proposed method results in natural out-of-sample predictions, discussed in the next section.

Supervised variants of manifold embedding have also been proposed when class labels are available in training data, including for the Laplacian Eigenmaps [68, 46, 61]. The basic idea is to learn a low-dimensional embedding of the data according to the constructed adjacency matrix that also corresponds to a good separation of classes, and then use the coordinates in this embedding as predictors instead of the original variables. For general response variables instead of class labels, there is no supervised variant of Laplacian Eigenmaps. More importantly, the embedding coordinates are typically complicated implicit functions of all the variables, and their coefficients cannot be interpreted in any meaningful way. Our method, on the other hand, has the original variables as predictors in the model (and nothing else), and thus their regression coefficients are readily interpretable.

2.6 Prediction and choosing the tuning parameter

To predict future response values on the training individuals, which is called the “in-sample prediction task”, we simply use $\hat{\alpha} + X\hat{\beta}$. In practice, it is more important to make out-of-sample prediction: predicting response variables on a group of new subjects whose covariate as well as the network connections are not observed when estimating the model. Since we have a different α_v for each node v , predicted individual effects are needed for predicting the responses for a group of n' new samples, denoted by α_1 . Note that now we have an enlarged network with $n + n'$ nodes. Assume the associated Laplacian for the enlarged network is

$$L' = \begin{bmatrix} L_{11} & L_{12} \\ L_{21} & L_{22} \end{bmatrix},$$

where L_{11} corresponds to the positions of the n' test samples and L_{22} corresponds to the positions of the original n training samples. To make prediction of individual effects on new samples given the ones in the training set, we minimize the network cohesion penalty fixing $\hat{\alpha}$:

$$\min_{\alpha_1} (\alpha_1, \hat{\alpha})^T L' (\alpha_1, \hat{\alpha}).$$

This gives

$$\hat{\alpha}_1 = -L_{11}^{-1} L_{12} \hat{\alpha}.$$

This process is equivalent to estimating the RNC estimator (2) on the enlarged network, fixing the training estimation. As the response for the new samples are not observed, only the cohesion penalty is involved. There is another type of prediction task that is studied a lot in semi-supervised learning literature [70] lying between in-sample prediction and out-of-sample prediction, in which the network connections of test samples are already observed in training procedure, but the covariates are not observed. In such situation, we can include all individual effects in the cohesion penalty when estimating the model and then follow the in-sample prediction procedure.

The tuning parameter λ can be selected by cross-validation. Randomly splitting or sampling from a network is not straightforward and how to do this is, in general, an open problem; however, we found that the usual “naive” cross-validation finds very good tuning parameters for our method, perhaps because it is fundamentally a regression problem and we are not attempting to make any inferences about the structure of the network. We tune using regular 10-fold cross-validation, randomly splitting the samples into 10 folds, leaving each fold out in turn, and training the model using the remaining nine folds and the corresponding induced subnetwork. The cross-validation error is computed as the average of the prediction errors on the fold that was left out, and the tuning parameter is picked to minimize the cross-validation error.

2.7 An efficient computation strategy

Computing the estimator (4) involves solving a $(n + p) \times (n + p)$ linear system so a naive implementation would require $O((n + p)^3)$ operations. For GLMs, such a system has to be solved in each Newton step. This computational burden can be reduced significantly by taking advantage of the fact that most networks in practice have sparse adjacency matrices as well as sparse Laplacians, which allows for using block elimination. A general description of this strategy can be found in many standard texts (see e.g. [9], Ch. 4). Here we give the

details in our setting.

The linear system we need to solve is

$$(\tilde{X}^T \tilde{X} + \lambda M) \mathbf{a} = \mathbf{b}.$$

From (5), we can rewrite this system with the following block structure:

$$\begin{bmatrix} I + \lambda L & X \\ X^T & X^T X \end{bmatrix} \begin{bmatrix} \mathbf{a}_1 \\ \mathbf{a}_2 \end{bmatrix} = \begin{bmatrix} \mathbf{b}_1 \\ \mathbf{b}_2 \end{bmatrix}.$$

The top row gives

$$(I + \lambda L) \mathbf{a}_1 = (\mathbf{b}_1 - X \mathbf{a}_2)$$

and substituting this into the bottom row, we have

$$(X^T X - X^T (I + \lambda L)^{-1} X) \mathbf{a}_2 = \mathbf{b}_2 - X^T (I + \lambda L)^{-1} \mathbf{b}_1.$$

Note that $I + \lambda L$ is a symmetric diagonal dominant (SDD) matrix, and is sparse most of the time in practice, so $(I + \lambda L)^{-1} \mathbf{b}_1$ and $(I + \lambda L)^{-1} X$ can be efficiently computed [28, 16]. The cost of this step is roughly $O(p(n + 2|E|)(\log n)^{1/2})$, where $|E|$ is the number of edges in the network and c is some absolute constant. The cost of the remaining computations is dominated by the cost of inverting the $p \times p$ matrix $X^T X - X^T (I + \lambda L)^{-1} X$, which is of the same order as the cost of solving a standard least squares problem.

When A and L are dense matrices, with $|E| = O(n^2)$, the strategy above has the cost of $O(pn^2((\log n)^{1/2}))$, which is still better than naively solving the system, but we do not gain anything from block elimination unless L is sparse. However, we can first apply a graph sparsification algorithm to A and use the sparsified A^* as input for RNC. For instance, the algorithm of [55] can find A^* with $O(\epsilon^{-2} n \log n)$ edges at the cost of $O(|E| \log^2 n)$ operations such that its sparsified Laplacian L^* satisfies

$$(1 - \epsilon)L \preceq L^* \preceq (1 + \epsilon)L,$$

for a given constant $\epsilon > 0$. After this sparsification step, the complexity of solving the linear system reduces to $O(pn \log^c n)$ for $c \leq 3$. In Section 3, we will provide theoretical guarantees for the accuracy of the RNC estimator based on L^* compared to that based on L .

Note that when the number of edges is in the order of $O(n^2)$, the sparsification step itself has complexity of $O(n^2 \log^c n)$, which is not necessarily cheaper than directly solving the original dense linear system using the SDD property. However, the advantage of sparsification becomes obvious when one has to iteratively solve the linear systems for the GLM or Cox's model, and/or compute a solution path for a sequence of λ values. In such situations, sparsification only has to be done once and the average complexity of solving the linear system can be close to $O(n \log^c n)$ for the whole estimation procedure. Details of complexity calculations for the RNC are given in Appendix B; a more comprehensive discussion of the computational trade-off of sparsification can be found in [49].

3 Theoretical properties of the RNC estimator

Recall the RNC estimator is given by

$$\hat{\boldsymbol{\theta}} = (\tilde{X}^T \tilde{X} + \lambda M)^{-1} \tilde{X}^T \mathbf{Y}, \quad (11)$$

where

$$M = \begin{bmatrix} L & 0 \\ 0 & 0 \end{bmatrix}.$$

We continue to assume that X has centered columns and full column rank. Intuitively, we expect the network cohesion effect to improve prediction only when the network provides “new” information that is not already contained in the predictors X . We formalize this intuition in the following assumption:

Assumption 1. For any $\mathbf{u} \neq 0$ in the column space of X , $\mathbf{u}^T L \mathbf{u} > 0$.

This natural and fairly mild assumption is enough to ensure the existence of the RNC estimator. Write $\text{col}(X)$ for the linear space spanned by columns of X and $\text{col}(X)^\perp$ for its orthogonal complement. Then the projection matrix onto $\text{col}(X)^\perp$ is $P_{X^\perp} = I_n - P_X$, where $P_X = X(X^T X)^{-1} X^T$. Write $\lambda_{\min}(M)$ for the minimum eigenvalue of any matrix M . Then we have the following lemma:

Proposition 1. Whenever $\lambda > 0$, we have $0 \leq \nu = \lambda_{\min}(P_{X^\perp} + \lambda L) \leq 1$. Under Assumption 1 the RNC estimator (11) exists.

Lemma 1 in the Appendix shows that when the network is connected and X is centered, the RNC estimator always exists since in a connected graph, L has rank $n - 1$, and an eigenvector $\mathbf{1}$.

Theorem 1. Under Assumption 1, the RNC estimator $\hat{\boldsymbol{\theta}} = (\hat{\boldsymbol{\alpha}}, \hat{\boldsymbol{\beta}})$ defined by (11) satisfies

$$\text{MSE}(\hat{\boldsymbol{\alpha}}) \leq \frac{\lambda^2}{\nu^2} \|L\boldsymbol{\alpha}\|^2 + \frac{n}{\nu} \sigma^2, \quad (12)$$

$$\text{MSE}(\hat{\boldsymbol{\beta}}) \leq \frac{\lambda^2}{\nu^2 \mu} \|L\boldsymbol{\alpha}\|^2 + \sigma^2 \left(\frac{1}{\nu} + 1 \right) \text{tr}((X^T X)^{-1}), \quad (13)$$

$$\mathbb{E} \|\hat{\mathbf{Y}} - \mathbb{E} \mathbf{Y}\|^2 \leq \frac{\lambda^2}{\nu} \|L\boldsymbol{\alpha}\|^2 + \sigma^2 \|S_\lambda\|_F^2, \quad (14)$$

where the minimum eigenvalue of $X^T X$ is denoted by μ and $\|S_\lambda\|_F$ is the Frobenius norm of the shrinkage matrix $S_\lambda = \tilde{X}(\tilde{X}^T \tilde{X} + \lambda L)^{-1} \tilde{X}^T$. Moreover, when $\|L\boldsymbol{\alpha}\| = 0$, RNC is unbiased.

The proof is given in the Appendix where the expressions for exact errors are also available. Theorem 1 applies to any fixed n . The asymptotic results as the size of the network n grows are presented next in Theorem 2. We add the subscript n to previously defined quantities to emphasize the asymptotic nature of this result.

Theorem 2. If Assumption 1 holds, $\mu_n = O(n)$, $\|L_n \boldsymbol{\alpha}_n\|^2 = o(n^c)$ for some constant $c < 1$, and there exists a sequence of λ_n and a constant $\rho > 0$ such that $\liminf_n \nu_n > \rho$, then

$$\text{MSE}(\hat{\boldsymbol{\beta}}) \leq O(\lambda_n^2 n^{-(1-c)}) + O(n^{-1}).$$

Therefore if $\lambda_n^2 = o(n^{1-c})$, $\hat{\boldsymbol{\beta}}$ is an L_2 -consistent estimator of $\boldsymbol{\beta}$.

Remark 2. Note that the quantity $L\alpha$ appearing in the assumptions is the gradient of the cohesion penalty with respect to α , $\nabla_\alpha \alpha^T L\alpha = 2L\alpha$. We call $L\alpha$ the cohesion gradient. In physics, cohesion gradient is used to measure heat diffusion on graphs when α is a heat function:

$$(L\alpha)_v = |N(v)| \left(\alpha_v - \frac{\sum_{u \in N(v)} \alpha_u}{|N(v)|} \right).$$

where $N(v)$ is the set of neighbors of v defined by the graph. Thus $\|L\alpha\|$ represents the difference between nodes' individual effects and the average of their neighbors' effects. The condition of Theorem 2 requires that the norm of the vector $L\alpha \in \mathbb{R}^n$ grows slower than $O(\sqrt{n})$. This is not hard to satisfy in many networks. One example is shown by the following proposition.

Proposition 2. Assume the network given is a $\sqrt{n} \times \sqrt{n}$ lattice network. Then $\|L\alpha\|^2 \leq n^c$ as long as α is in the subspace spanned by k smallest eigenvalues of L for some $k \leq Cn^{\frac{1+c}{2}}$, where C and c are some constants and $c < 1$.

It is instructive to compare the MSE of our estimator with the MSE of the ordinary least squares (OLS) estimator as well as its noninformative generalization - the null model. For OLS, we have

$$\hat{\beta}_{OLS} = (X^T X)^{-1} X^T \mathbf{Y}, \quad \hat{\alpha}_{OLS} = \bar{y} \mathbf{1},$$

which does not enforce network cohesion. Here $\hat{\alpha}_{OLS}$ is the common intercept. The RNC estimator reduces bias caused by the network-induced dependence among samples and as a trade-off increases variance; thus intuitively, one would expect that the signal-to-noise ratio and the degree of cohesion in the network will determine which estimator performs better. From Theorem 1 and the basic properties of the OLS estimator (stated as Lemma 1 in the Appendix), it is easy to see that if

$$\left(\frac{n}{\nu} - 1 \right) \sigma^2 \leq V(\alpha) - \frac{\lambda^2}{\nu^2} \|L\alpha\|^2 \quad (15)$$

where $V(\alpha) = \sum_v (\alpha_v - \bar{\alpha})^2$, then the RNC estimator of the individual effects $\hat{\alpha}$ has a lower MSE than that of $\hat{\alpha}_{OLS}$. The left hand side of (15) represents the increase in variance induced by adding the network penalty, whereas the right hand side is the corresponding reduction in squared bias. When α is smooth enough over the network, $\|L\alpha\|$ is negligible compared to other terms, and the condition essentially requires that the total variation of α_v around its average is larger than the total noise level. Similarly, for the coefficients β , if

$$\text{tr}((X^T X)^{-1}) \frac{\sigma^2}{\nu} \leq \|(X^T X)^{-1} X^T \alpha\|^2 - \frac{\lambda^2}{\mu} \|L\alpha\|^2 \quad (16)$$

then the RNC estimator $\hat{\beta}$ has a lower MSE than $\hat{\beta}_{OLS}$. Again, the two sides of the inequality represent the increase in variance and the reduction in squared bias, respectively. The comparison with estimates from the null model remains identical for β , due to the fact that it equals to $\hat{\beta}_{OLS}$. The comparison with null model in α can be similarly done but the format is more complicated as that involves another tuning parameter for the null model, so we will not give the formula here. However, we will show such comparison in MSPE with OLS and null model in the next example.

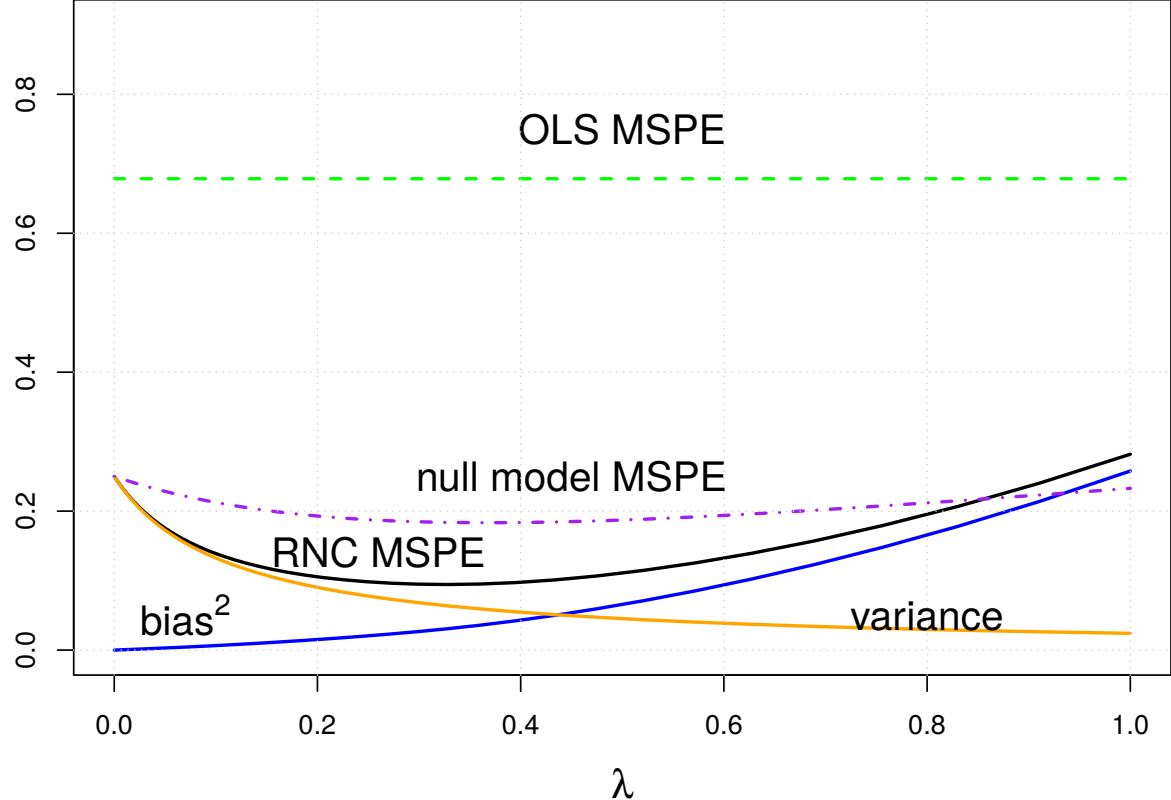


Figure 1: Mean squared prediction error $\mathbb{E}\|\hat{\mathbf{Y}} - \mathbb{E}\mathbf{Y}\|^2/n$ and the bias-variance trade-off of the RNC estimator (based on the upper bound (14) in Theorem 1), in the setting of Example 1 with $\sigma = 0.5$.

Example 1. We illustrate the bias-variance trade-off on a simple example. Suppose we have a network with $n = 300$ nodes which consists of three disconnected components G_1, G_2, G_3 , of 100 nodes each. Each component is generated as an Erdos-Renyi graph, with each pair of nodes forming an edge independently with probability 0.05. Individual effects α_i are generated independently from $\mathcal{N}(\eta_{c_i}, 0.1^2)$, where $c_i \in \{1, 2, 3\}$ is the component to which nodes i belongs, $\eta_1 = -1$, $\eta_2 = 0$, $\eta_3 = 1$. We set $\lambda = 0.1$. Substituting the expectation EA for A , we have $\nu \approx 0.5$, $\|L\alpha\|^2 \approx 105$, and $V(\alpha) \approx 203$. Then as long as the noise variance $\sigma < 0.57$, (15) will be satisfied. Similarly, $X^T X \approx nI_2$, and $\|X^T \alpha\|^2 \approx 406$ in expectation. Thus (16) holds and the RNC is beneficial if $\sigma < 0.54$ (approximately). The bias-variance trade-off in the mean squared prediction errors (MSPE) can be demonstrated explicitly when varying λ ; Figure 1 shows this trade-off between bias and variance together with the OLS baseline when $\sigma = 0.5$. The MSPEs of OLS and the null model are also shown. Note that this calculation for RNC is based on conservative bounds. In reality the RNC is going to be beneficial for a larger range of σ values.

Remark 3. If we use (6) and are willing to make strong assumptions about the distribution as in the Bayesian interpretation, it can be shown (see [50], Ch. 7 for details) that $\hat{\alpha}$ is the best linear unbiased predictor (BLUP) of α and $\hat{\beta}$ is the best linear unbiased estimator (BLUE) of β . Nevertheless, we believe such assumptions are almost always too strong in reality thus will not give more discussions in that direction.

Finally, we investigate the effects of graph sparsification, proposed in Section 2.7 to reduce computational cost, on the properties of the RNC estimator. For any $\epsilon > 0$, let L^* be the

Laplacian of a network on the same nodes satisfying

$$(1 - \epsilon)L \preceq L^* \preceq (1 + \epsilon)L. \quad (17)$$

In addition, let $\hat{\boldsymbol{\theta}}$ be the minimizer of

$$f(\boldsymbol{\theta}) = \ell(\boldsymbol{\alpha} + X\boldsymbol{\beta}; \mathbf{Y}) + \lambda\boldsymbol{\alpha}^T L\boldsymbol{\alpha}, \quad (18)$$

and $\hat{\boldsymbol{\theta}}^*$ be the minimizer of

$$f^*(\boldsymbol{\theta}) = \ell(\boldsymbol{\alpha} + X\boldsymbol{\beta}; \mathbf{Y}) + \lambda\boldsymbol{\alpha}^T L^*\boldsymbol{\alpha}, \quad (19)$$

where ℓ can be a general loss function, such as the sum of squared errors in linear model or the negative log-likelihood in GLM.

Theorem 3. Given two Laplacians L and L^* satisfying (17) for $0 < \epsilon < 1/2$, assume ℓ in (18) is twice differentiable and f is strongly convex with $m > 0$, such that for any $\boldsymbol{\theta} = (\boldsymbol{\alpha}, \boldsymbol{\beta}) \in \mathbb{R}^{n+p}$,

$$\nabla^2 f(\boldsymbol{\theta}) \succeq mI_{n+p}.$$

Then $\hat{\boldsymbol{\theta}}$ and $\hat{\boldsymbol{\theta}}^*$ minimizing (18) and (19) respectively, with the same λ , satisfy

$$\|\hat{\boldsymbol{\theta}}^* - \hat{\boldsymbol{\theta}}\|^2 \leq \frac{2\epsilon\lambda}{m} \min \left(2\hat{\boldsymbol{\alpha}}^T L\hat{\boldsymbol{\alpha}} + |\hat{\boldsymbol{\alpha}}^T L\hat{\boldsymbol{\alpha}} - \hat{\boldsymbol{\alpha}}^{*T} L^* \hat{\boldsymbol{\alpha}}^*| + 2\epsilon\hat{\boldsymbol{\alpha}}^{*T} L^* \hat{\boldsymbol{\alpha}}^*, \frac{2\epsilon\lambda}{m} \lambda_1(L)^2 \|\hat{\boldsymbol{\alpha}}\|^2 \right). \quad (20)$$

The proof is given in the Appendix. Theorem 3 is a generalization of the result [49] for point estimation by Laplacian smoothing (or kriging) for Gaussian and binary data. Our bound is slightly better than that of [49].

Remark 4. The term $\hat{\boldsymbol{\alpha}}^T L\hat{\boldsymbol{\alpha}}$ is the cohesion penalty and is expected to be small for estimated $\hat{\boldsymbol{\alpha}}$. Further, we can expect both $|\hat{\boldsymbol{\alpha}}^T L\hat{\boldsymbol{\alpha}} - \hat{\boldsymbol{\alpha}}^{*T} L^* \hat{\boldsymbol{\alpha}}^*|$ and $\epsilon\hat{\boldsymbol{\alpha}}^{*T} L^* \hat{\boldsymbol{\alpha}}^*$ to be much smaller than $\hat{\boldsymbol{\alpha}}^T L\hat{\boldsymbol{\alpha}}$, and the first bound in (20) is typically much smaller than the second. Therefore, the bound is essentially

$$\|\hat{\boldsymbol{\theta}}^* - \hat{\boldsymbol{\theta}}\|^2 \lesssim \frac{4\epsilon\lambda}{m} \hat{\boldsymbol{\alpha}}^T L\hat{\boldsymbol{\alpha}}. \quad (21)$$

Remark 5. The theorem shows that the squared error in estimation with an ϵ -approximated Laplacian is decreasing linearly in ϵ . In particular, it is easy to check that for the linear regression case, we have

$$\nabla^2 \ell(\boldsymbol{\theta}) = 2(\tilde{X}^T \tilde{X} + \lambda M).$$

Strong convexity always holds whenever RNC estimate exists, and the bound becomes

$$\|\hat{\boldsymbol{\theta}}^* - \hat{\boldsymbol{\theta}}\|^2 \lesssim \frac{2\epsilon\lambda\hat{\boldsymbol{\alpha}}^T L\hat{\boldsymbol{\alpha}}}{\lambda_n(\tilde{X}^T \tilde{X} + \lambda M)}. \quad (22)$$

4 Numerical performance evaluation

In this section, we investigate the effects of including network cohesion on simulated data, using both linear regression and logistic regression as examples.

The networks are generated from the stochastic block model with $n = 300$ nodes and $K = 3$

blocks. Under the stochastic block model, the nodes are assigned to blocks independently by sampling from a multinomial distribution with parameters (π_1, \dots, π_K) . Then given block labels c_i for $i = 1, \dots, n$, the edges A_{ij} , $1 \leq i < j \leq n$, are generated as independent Bernoulli variables with $P(A_{ij} = 1) = B_{c_i c_j}$, where the $K \times K$ symmetric matrix B contains probabilities of within-block and between-block connections. We set $\pi_1 = \pi_2 = \pi_3 = 1/3$, $B_{kk} = p_w = 0.2$, $B_{kl} = p_b = 0.02$ for all $k \neq l$.

As in Example 1, the individual effects α_i 's are generated independently from a normal distribution with the mean determined by the node's block, $\mathcal{N}(\eta_{c_i}, s^2)$, where $\eta_1 = -1$, $\eta_2 = 0$, $\eta_3 = 1$, and the parameter s controls how close the α_i 's within each block are. The smaller s is, the more cohesion we expect in the network. The predictor coefficients β are drawn independently from $\mathcal{N}(1, 1)$. Note that we are testing RNC in a misspecified model in the following sense 1) the between block edges are actually false information to the network cohesion assumption; 2) even for connected nodes in the same block, the pairwise differences are from random noises, thus the smoothness requirement of Theorem 2 clearly does not hold except when $s = 0$.

On top of the baseline method (OLS for continuous response and logistic regression for binary response), we include two additional methods for comparison: the null model, where the graph is empty and we simply add a ridge penalty on the individual effects, and a fixed effects model which uses the same α for all the nodes in the same block. Note that the latter is an oracle model in the sense that it uses the true block memberships which are not known in practice. In all of our examples, we always select tuning parameters by 10-fold cross-validation. However, in this specific example, the linear null model cannot be selected in this way. This is because its out-of-sample prediction is always identical to that of OLS as shown in Lemma 3 in appendix, whatever λ to be used in (7). This already indicates its (and the standard mixed models') difficulty in making out-of-sample predictions. Therefore in this specific example, we select λ of the null model using the restricted maximum likelihood (REML) estimate under the corresponding linear mixed model framework. Specifically, we use the REML estimate of $\lambda = \sigma^2/\zeta^2$, in the Bayesian interpretation and the rest is the same as what we discussed previously.

Four performance metrics are used: the average versions MSE of α , β , in-sample MSPE and out-of sample MSPE, defined by $\frac{1}{n}\|\hat{\alpha} - \alpha\|^2$, $\frac{1}{p}\|\hat{\beta} - \beta\|^2$, $\frac{1}{n}\mathbb{E}\|\hat{\mathbf{Y}} - \mathbb{E}\mathbf{Y}\|^2$, and $t \frac{1}{n_t}\mathbb{E}\|\hat{\mathbf{Y}}_t - \mathbf{Y}_t\|^2$ respectively, where $\hat{\mathbf{Y}}_t$ is a vector of observations on $n_t = 50$ nodes that is generated in the same model but not used in estimating the models.

Figure 2 shows the results of the four metrics when we vary s from 0 to 1. When s is very small, the oracle fixed effects model performs best, since it is very close to the true model. RNC is the second best in this situation. As s increases, the true signals of the network are overwhelmed by noises and every method becomes worse. Regarding the estimation of α , the increasing s makes α more like independent Gaussian noises thus the null model adapts better in estimating α as s becomes large. RNC, on the other hand, lies between the oracle fixed effects model which purely relies on the network information and the null model model, which assumes pure noisy α . When it comes to the estimation of β , the oracle fixed effects model is always the best and RNC is very close to it, while OLS and null model are much inferior. The pattern of in-sample-prediction errors is similar to that of estimating α . For out-of-sample prediction, again the oracle model does the best and RNC is very close to it. The null model is identical to OLS and is much worse for all s values. While one might argue that the oracle block information could be replaced by estimated communities in the network, for which many methods are available, this would only help if

the underlying model does indeed have communities. The RNC, on the other hand, does not require an assumption on communities and can adapt to cohesion over many different types of underlying graphs.

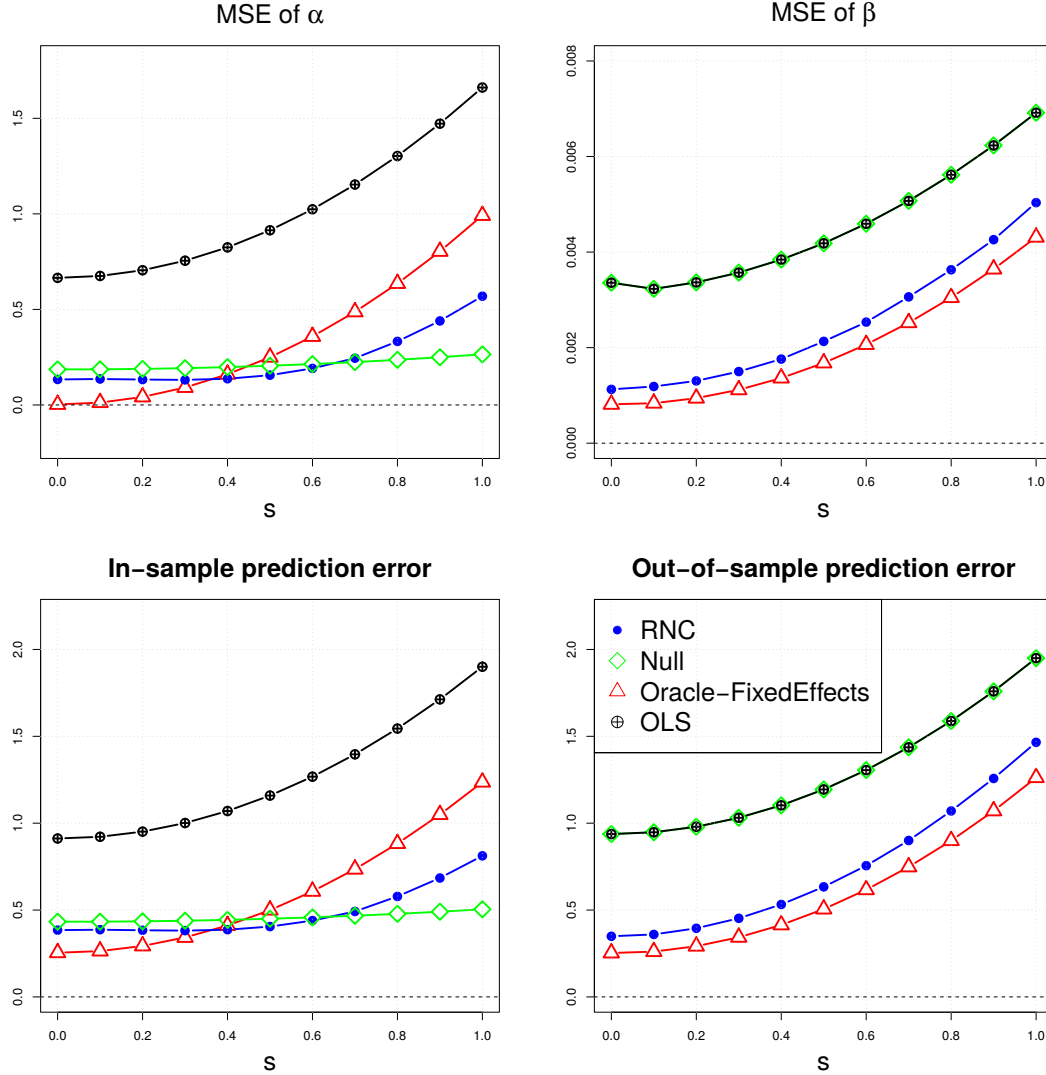


Figure 2: Performance of four linear regression methods, measured by the MSE of α , β , in-sample mean squared prediction errors and out-of-sample prediction errors.

Next, we use the same setting for generating the network, covariates, and parameters, but instead of taking Y to be Gaussian, we generate \mathbf{Y} from the Bernoulli distribution with probabilities of success given by the logit of $\mathbf{X}^T \boldsymbol{\beta} + \boldsymbol{\alpha}$. We then estimate the parameters by the usual logistic regression and by a logistic regression with our proposed network cohesion penalty. We fix a small value of the ridge regularization tuning parameter, $\gamma = 0.01$, as we only use this for numerical stability. Similarly as before, we compare the methods by computing the average MSE of $\boldsymbol{\alpha}$, $\boldsymbol{\beta}$, and the average MSE on the vector of n Bernoulli probabilities estimated by

$$\hat{p}_i = \frac{\exp(\mathbf{x}_i^T \hat{\boldsymbol{\beta}} + \hat{\alpha}_i)}{1 + \exp(\mathbf{x}_i^T \hat{\boldsymbol{\beta}} + \hat{\alpha}_i)},$$

as well as the probabilities of 50 hold-out samples. The latter two are treated by analogy

of in-sample and out-of-sample prediction errors.

Figure 3 shows the average MSE of α , β , and in-sample and out-of-sample probabilities. The null provides a small improvement over standard logistic regression in estimating α , β and in-sample-probability but does a similar job in making out-of-sample predictions, a pattern that coincides with what we observed in linear regression settings. Similarly to linear regression, the cohesion penalty using oracle groups makes the largest gains at small s , when the cohesion is highest. The logistic RNC also performs best for smaller s , and while it does not come as close to the oracle as it does in the linear case, it uniformly outperforms the other non-oracle methods, and as s becomes large, adapting better to a lesser degree of cohesion than the oracle with its fixed groups does.

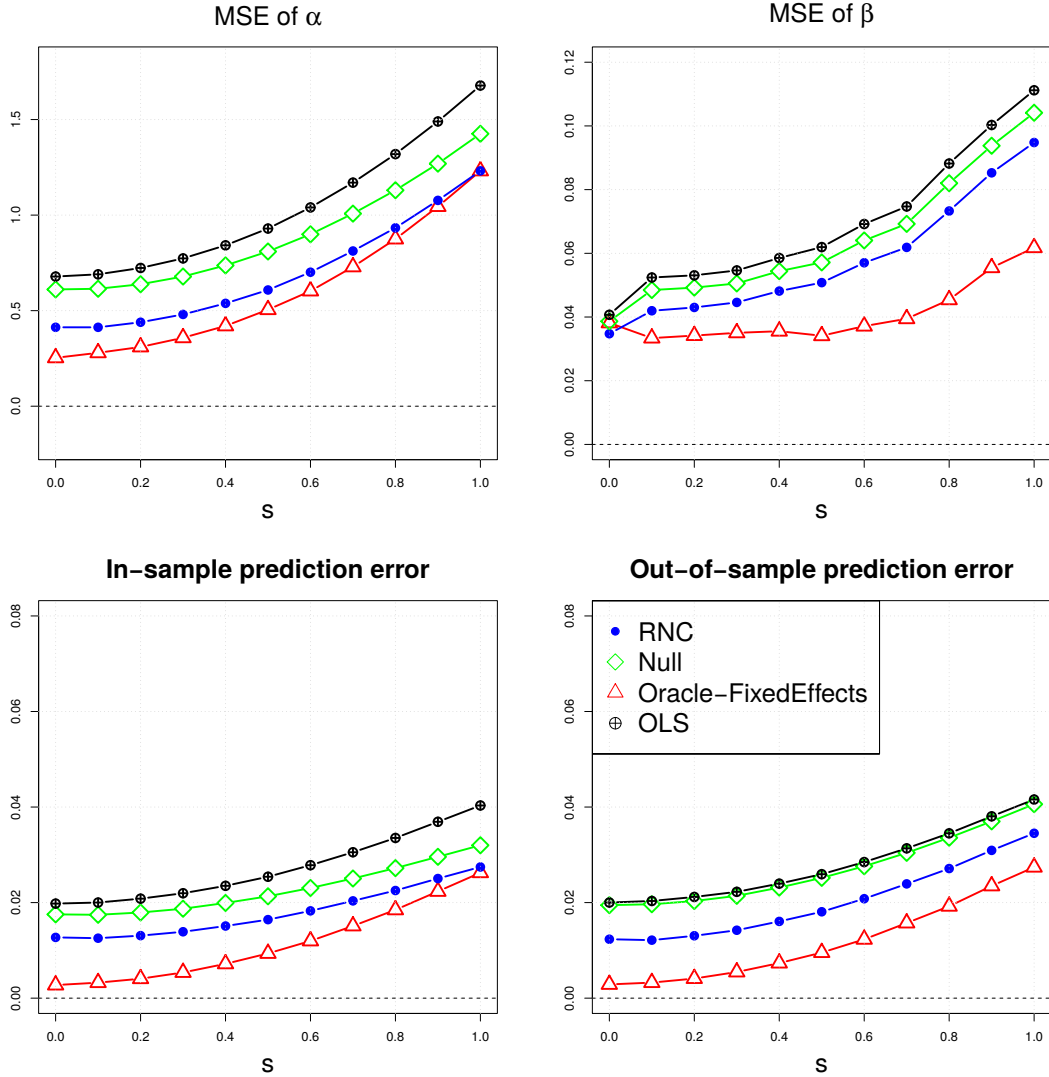


Figure 3: Performance of four logistic regression methods, measured by the MSE of α , β , in-sample mean squared prediction errors and out-of-sample prediction errors.

Sparsified adjacency matrix

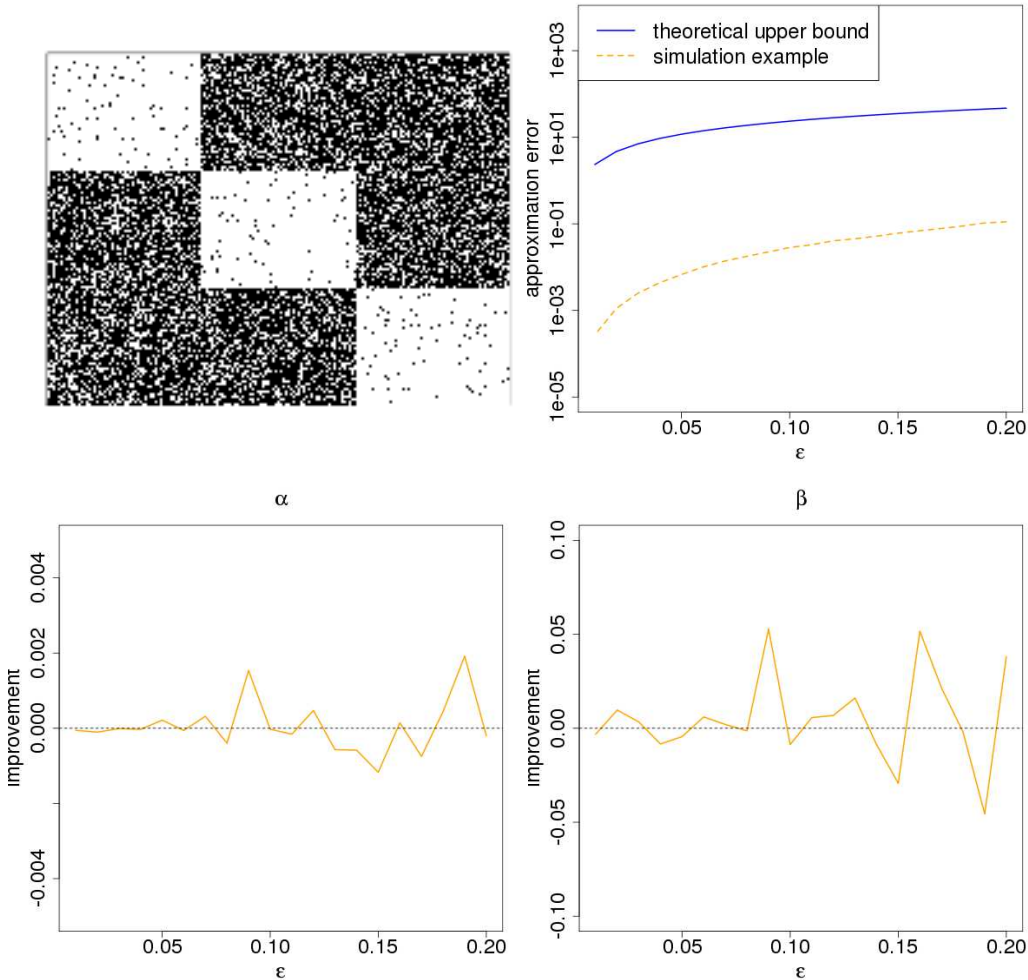


Figure 4: Top left: the adjacency matrix of the sparsified network for $\epsilon = 0.15$ (white indicates a nonzero entry, black is a zero entry); Top right: $\|\hat{\theta}^* - \hat{\theta}\|^2$ and the bound (22); Bottom left: relative improvement of the sparsified estimator α^* over the original estimator $\hat{\alpha}$, that is, $1 - \text{MSE}_{\alpha^*}/\text{MSE}_{\hat{\alpha}}$; Bottom right: relative improvement of the sparsified estimator β^* over the original estimator $\hat{\beta}$.

We conclude this section with a simple example illustrating the graph sparsification approach to dense networks. We generate a weighted network with $n = 3000$ nodes, divided into three blocks of 1000 nodes each. All the within-block entries of the weighted adjacency matrix are 1 and the other entries are 0.1. Thus the network matrix is a fully dense matrix. The other settings are the same as we used in the linear regression simulation, and we compare the linear RNC estimator estimated using the original Laplacian L to the one based on the sparsified L^* . Figure 4 shows the results as a function for different values of the approximation accuracy ϵ 's, defined in (17). The top left plot shows the the sparsified matrix corresponding to $\epsilon = 0.1$, which has around 52% of all elements set to 0. The top right plots shows the observed approximation error $\|\hat{\theta}^* - \hat{\theta}\|^2$ and its theoretical upper bound (22). The theoretical bound is conservative but follows the same trend. Finally, the bottom plots of the difference in estimation errors for α and β show that the difference between the sparsified and the original estimators goes to 0 as $\epsilon \rightarrow 0$, as it should, and that for moderate values of ϵ the differences are small and go in either direction, which suggests

an increase in variance but not much change in bias. Overall, in this example sparsification provides a reliable approximation to the original RNC estimator, and is a useful tool to save computational time for large dense networks.

5 Applications

In this section, we use our method to incorporate network effects and improve prediction in two applications using the data from the National Longitudinal Study of Adolescent Health (the AddHealth study) [23]. AddHealth was a major national longitudinal study of students in grades 7-12 during the school year 1994-1995, after which three further follow-ups were conducted in 1996, 2001-2002, and 2007-2008. We will only use Wave I data. In the Wave I survey, all students in the sample completed in-school questionnaires, and a follow-up in-home interview with more detailed questions was conducted for a subsample. There are questions in both the in-school survey and the in-home interview asking for friends nominations (up to 10), and we can construct friendship networks based on this information, ignoring the direction of nominations. The networks from the two surveys are different. We will consider two specific prediction tasks in this section. The first task, considered by [10], is predicting students' recreational activity from their demographic covariates and their friendship networks, accomplished via a network autoregressive model in [10], who used the in-school survey data. In order to compare with our method directly, we also use the in-school data only for this task. Our second application is to predict the first time of marijuana use, via Cox's proportional hazard model. Since the data on marijuana use are only available from the in-home interview records, in the second application we will use the friendship network constructed from the in-home interviews as well.

5.1 Recreational activity in adolescents: a linear model example

In [10], social effects were incorporated into ordinary linear regression via the auto-regressive model

$$y_v = \frac{1}{|N(v)|} \sum_{u \in N(v)} (\gamma y_u + \mathbf{x}_u^T \boldsymbol{\tau}) + \mathbf{x}_v^T \boldsymbol{\beta} + \epsilon_v, v \in V. \quad (23)$$

The authors called this the social interaction model (SIM). In econometric terminology, the local average of responses models endogenous effects, and the local averages of predictors are the exogenous effects. When there are known groups in the data, fixed effects can be added to this model [32]. In [10], SIM was applied to the AddHealth data to predict levels of recreational activity from a number of demographic covariates as well as the friendship network. The covariates are age, grade, sex, race, born in the U.S. or not, living with the mother or not, living with the father or not, mother's education, father's education, and parents' participation in the labor market. For some of the categorical variables, some levels were merged; refer to [10] for details. The recreational activity was measured by the number of clubs or organizations of which the student is a member, with "4 or more" recorded as 4. The histogram as well as the mean and standard deviation of recreational activity are shown in Figure 5. We used exactly the same variables with the same level merging.

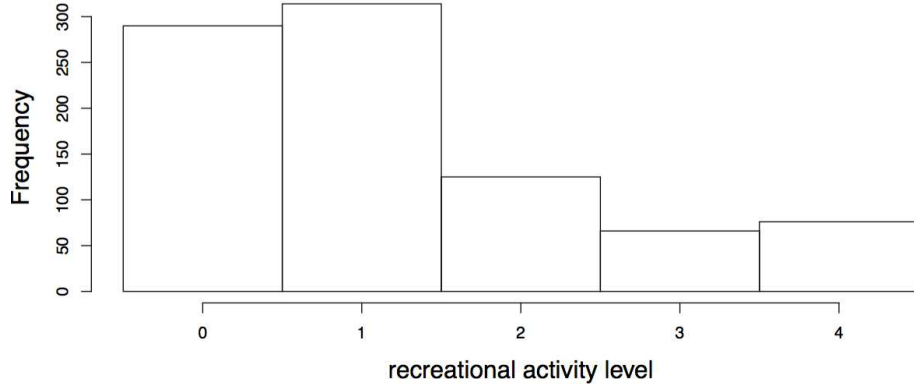


Figure 5: Histogram of the response, recreational activity level, from the data set used in the linear regression example. The data has mean value 1.224 and standard deviation 1.231.

We compare performance of our proposed RNC method with the SIM model (23) from [10], and to regular linear regression without network effects implemented by ordinary least squares (OLS), with the same response and predictors as in [10]. The null model again gave results nearly identical to the OLS. We use the largest school in the dataset, where, after deleting records with missing values for the variables we use, the network has 1995 students. To see the effect of additional predictors, we include the variables in the model one at a time following the standard forward selection algorithm with OLS. To avoid underestimating prediction errors, we use the largest connected component of the network as our prediction evaluation data, with 871 nodes and the average degree of 3.34. The remaining 1124 samples are used for variable selection to determine the order of variables to be added to the model. After deleting students with missing values, all the rest were living with both parents so we omit those two variables from further analysis.

To evaluate predictive performance, we randomly hold out 80 students from the largest connected component as test data, and fit all the models using the rest. The order in which the variables are added to the models is fixed in advance using the separate variable selection dataset and is the same for all models. The mean squared prediction errors on the 80 students are averaged over 50 independent random data splits into training and test sets. The RMSEs over these 50 splits are shown in Table 1. In each row, the differences between the three models are all statistically significant with a p -value of less than 10^{-4} using a paired t -test over the 50 random splits. It is clear that both SIM and RNC are able to improve prediction by using the network information, but RNC is more effective at this than SIM.

Note that none of the predictors are very strong, and the network information is relatively more helpful: e.g., the RNC error using only the network cohesion correction and no predictors at all is lower than the error of *any* model fitted by either OLS or SIM. As with any other prediction task, adding unhelpful covariates tends to slightly corrupt performance, and all models achieve their best performance using the first three variables (mother's education, born in the US, and race).

Table 1: Root mean squared errors for predicting students’ recreational activity level. The average is taken over 50 independent data splits, in each of which 80 samples are randomly chosen to be test set. All differences across rows are statistically significant with a p -value $< 10^{-4}$ as measured by a paired t -test. The model in each row includes all the variables from previous rows.

model	OLS & Null	SIM	RNC
no covariates	1.235	1.185	1.163
+ mother’s education	1.231	1.183	1.159
+ born in the US	1.231	1.180	1.162
+ race	1.213	1.173	1.154
+ father’s education	1.215	1.179	1.160
+ sex	1.214	1.178	1.158
+ age	1.215	1.176	1.157
+ grade	1.214	1.176	1.157
+ parents in labor market	1.215	1.177	1.158

5.2 Predicting the risk of adolescent marijuana use

This application illustrates the benefits of network cohesion in the setting of survival analysis. While prediction of continuous or categorical responses on networks is common, there are settings where survival analysis is more appropriate. In the AddHealth survey, the students were asked “How old were you when you tried marijuana for the first time?”, and the answer can either be age (an integer up to 18) or “never”. The students who say “never” should be treated as censored observations, and modeling the time until a student tries marijuana for the first time in a survival model is more appropriate than treating this as a continuous response in a linear model. Here we apply Cox’s proportional hazard model with network cohesion regularization to the largest community in the dataset with 1862 students from the Wave I in-home interview (this question was only asked in the in-home interviews). The friendship network is also based on friend nominations from in-home data for consistency, and there are 2820 additional covariates on each student collected from the in-home surveys. In order to illustrate the benefits of network cohesion on concrete models, we first select a small subset of variables that can act as informative covariates. To do this, we split the data roughly into 2/3 for variable selection, and 1/3 for fitting the proportional hazard model. Specifically, we randomly set aside 500 students, and took the largest connected component among the remaining 1362 students to fit the hazard model. This largest connected component consists of 668 nodes and has the average node degree of 2.83. All the remaining 1194 students were used for variable selection. The baseline we compare with is the regular Cox’s model since the SIM model does not extend to the survival setting. Again, the null RNC gives results almost identical to the regular Cox model.

For variable selection, we first order covariates by their p -values from fitting the regular univariate Cox’s model with that single covariate. Then we pick five most significant covariates with the requirement that each survey category (survey questions were grouped into categories) has no more than one variable selected, and the selected variable has no missing values in the 668 samples. We then use a regular forward selection algorithm to determine the order in which these five variables should be added to the model, and compare the five models chosen by forward selection. Note that with the network cohesion penalty, we can still fit the model with no covariates and individual hazards only, but this is not possible for the regular Cox’s model since the partial likelihood is not defined without covariates. In addition, we also include a naive extension of the social interaction model (SIM) from

linear regression problem. Specifically, we include all neighborhood average of covariates that are used by the regular Cox’s model in SIM and still fit it as a Cox’s model. Compared to the regular Cox’s model, SIM doubles the number of covariates. Notice that in linear regression, SIM also has the autoregressive component on the response. But it is not clear how to define it in censored response so we do not include it in this setting.

Evaluating predictive performance in Cox’s model is not straightforward since the nonparametric h_0 in (9) is not estimated and the partial log-likelihood is not separable. We use the metric of [59, 65] to measure the prediction power. Suppose we have a training set and all quantities associated with it labeled (1), and a test set labeled (2). Let $\hat{\alpha}_{(1)}, \hat{\beta}_{(1)}$ be the estimates of α and β on the training set. The predictive partial log-likelihood (PPL) for the test set is calculated as

$$\ell_{(1+2)}(\hat{\alpha}_{(1)}, \hat{\beta}_{(1)}) - \ell_{(1)}(\hat{\alpha}_{(1)}, \hat{\beta}_{(1)})$$

where $\ell_{(1+2)}$ is the partial log-likelihood evaluated on all samples (both training and test), and $\ell_{(1)}$ is the partial log-likelihood evaluated only on the training samples. When ℓ is a log-likelihood separable across individuals, this gives exactly the predictive log-likelihood in the usual sense. In our evaluation, we randomly select 60 nodes as the test set and use the remaining nodes and their induced sub-network as the training set. This is independently repeated 50 times and we use the average PPL of the 50 replications as the performance measure. For simplicity of comparisons, we fixed the value of tuning parameter $\lambda = 0.005$ for all models based on validation on a different school, and set $\gamma = 0.1$. This is a conservative approach to comparing our method with the regular Cox’s model, since tuning each model separately for RNC can only improve its performance.

Table 2: Average predictive partial log-likelihood (PPL) for the five models chosen by forward selection on a hold-out sample. The average is taken over 50 random splits of the data into 60 test samples and 608 training samples. In the parentheses are the p -values of the paired t -test between the PPL of the corresponding model (Cox or SIM) and RNC. The model in each row includes all the variables from previous rows.

model	Cox & Null	SIM	RNC
no covariates	—	—	-156.40
+ received school suspension	-157.43 ($< 10^{-8}$)	-156.46 (0.0010)	-155.63
+ has driven a car	-158.05 ($< 10^{-8}$)	-156.93 (0.6×10^{-3})	-156.03
+ illegal drugs easily available at home	-157.82 ($< 10^{-8}$)	-156.74 (0.0035)	-155.97
+ has a permanent tattoo	-156.68 (2.7×10^{-5})	-155.71 (0.37)	-155.46
+ speaks English at home	-156.66 (3.1×10^{-5})	-155.66 (0.48)	-155.47

Table 2 shows the average PPL after adding each variable to the model and the p -values from paired t -tests on the difference between regular Cox’s model/SIM and Cox’s model regularized by network cohesion. The model using the network information always does better than the same model without the network. RNC with no covariates is already somewhat better than the regular model with all the covariates, and RNC with just the first variable is better than any of the regular models or SIM.

We still want to know whether the improvements brought by RNC are practically significant, though they are mostly statistically significant in p -values. It is not straightforward to measure the magnitude of PPL as it is calculated from a partial log likelihood function. Nevertheless, we can take an intuitive measure of it by comparing the difference between numbers in the same column. The predictor “having a permanent tattoo” turns out to

be the covariate that gives the largest improvement on prediction, resulting in 1.14, 1.03 and 0.51 improvement on PPL for regular Cox's, SIM and RNC respectively. Adding any other single covariate never result in more than 0.25 PPL improvement. In contrast, the improvements of RNC over SIM in the same rows are 0.83, 0.9, 0.77, 0.25, 0.19 respectively. So intuitively, the improvement of RNC over SIM is similar to or even larger than adding a strong predictor in the model (recall that the predictors are the top five from the forward selection procedure). Finally, notice that SIM is much harder to interpret than RNC due to the usage of neighborhood average.

Using the complete network, the predicted individual effects range from -0.588 to 1.22. That means for the subject with the highest potential risk for marijuana usage, the individual hazard is about 3.4 times of the population baseline hazard. The estimated individual hazards $\exp(\hat{\alpha}_v)$'s are shown in Figure 6, represented by node size, together with the friendship network and the observed age when one first tried marijuana, represented by node color. One can see the cohesion effect in both the data itself and in the estimated hazards.

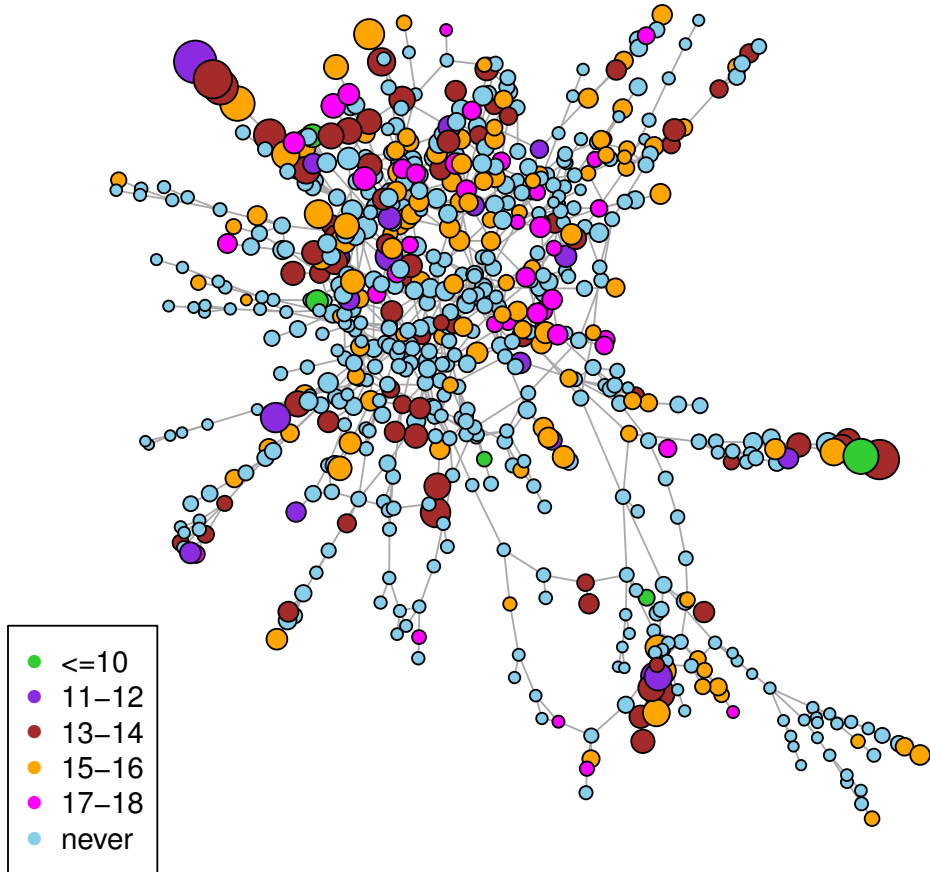


Figure 6: The friendship network of data set for marijuana risk prediction. Node size represents its estimated individual hazard for using marijuana, and node color the observed age when the student first tried marijuana.

6 Discussion

We have proposed a general framework for introducing network cohesion effects into prediction problems, without losing the interpretability and meaning of the original prediction models and in a computationally efficient manner. In a regression setting, we have also demonstrated theoretically when this approach will outperform regular regression and have shown the proposed estimator is consistent. In general, we can view this setting as another example of benefits of regularization when there are more parameters than one can estimate with the data available. Encouraging network cohesion implicitly reduces the number of free parameters that effectively need to be estimated, somewhat in the same spirit as the fused lasso penalty [57]. There are important differences, however; here we have a computationally efficient way to use the available network data and can explicitly assess the trade-off in bias and variance that results from encouraging cohesion. Another direction to explore is understanding the behavior of network cohesion on different kinds of networks. This can be accomplished if we leverage the large literature on random graph models for networks and instead of treating the network as given and fixed, model it as a realization of a network model with certain structure. Alternatively, one could analyze the effects on cohesion of certain network properties (degree distribution, communities, etc) implied by the properties of the graph Laplacian. While we focused on prediction in this paper, the cohesion penalty may also turn out to be useful in causal inference on networks when such inference is possible.

Acknowledgements

This research uses data from Add Health, a program project designed by J. Richard Udry, Peter S. Bearman, and Kathleen Mullan Harris, and funded by a grant P01-HD31921 from the Eunice Kennedy Shriver National Institute of Child Health and Human Development, with cooperative funding from 17 other agencies. Special acknowledgment is due Ronald R. Rindfuss and Barbara Entwistle for assistance in the original design. Persons interested in obtaining Data Files from Add Health should contact Add Health, The University of North Carolina at Chapel Hill, Carolina Population Center, 206 W. Franklin St., Chapel Hill, NC 27516-2524 (addhealth_contractsunc.edu). No direct support was received from grant P01-HD31921 for this analysis. This research was partially supported by NSF grants DMS-1159005 and DMS-1521551 (to E. Levina), NSF grant DMS-1407698 and NIH grant R01GM096194 (to J. Zhu), and a Rackham International Student Fellowship (to T. Li).

References

- [1] A. A. Amini, A. Chen, P. J. Bickel, and E. Levina. Pseudo-likelihood methods for community detection in large sparse networks. *The Annals of Statistics*, 41(4):2097–2122, 2013.
- [2] S. Asur and B. A. Huberman. Predicting the future with social media. In *Web Intelligence and Intelligent Agent Technology (WI-IAT), 2010 IEEE/WIC/ACM International Conference on*, volume 1, pages 492–499. IEEE, 2010.
- [3] M. Belkin and P. Niyogi. Laplacian eigenmaps for dimensionality reduction and data representation. *Neural computation*, 15(6):1373–1396, 2003.

- [4] M. Belkin, P. Niyogi, and V. Sindhwani. Manifold regularization: A geometric framework for learning from labeled and unlabeled examples. *Journal of machine learning research*, 7(Nov):2399–2434, 2006.
- [5] Y. Bengio, J.-F. Paiement, P. Vincent, O. Delalleau, N. Le Roux, and M. Ouimet. Out-of-sample extensions for lle, isomap, mds, eigenmaps, and spectral clustering. *Advances in neural information processing systems*, 16:177–184, 2004.
- [6] J. Besag. Spatial interaction and the statistical analysis of lattice systems. *Journal of the Royal Statistical Society. Series B (Methodological)*, pages 192–236, 1974.
- [7] N. Binkiewicz, J. T. Vogelstein, and K. Rohe. Covariate assisted spectral clustering. *arXiv preprint arXiv:1411.2158*, 2014.
- [8] G. Bosilca, A. Bouteiller, A. Danalis, T. Herault, P. Lemarinier, and J. Dongarra. Dague: A generic distributed dag engine for high performance computing. *Parallel Computing*, 38(1):37–51, 2012.
- [9] S. Boyd and L. Vandenberghe. *Convex optimization*. Cambridge University Press, 2004.
- [10] Y. Bramoullé, H. Djebbari, and B. Fortin. Identification of peer effects through social networks. *Journal of Econometrics*, 150(1):41–55, 2009.
- [11] D. Cai, X. He, and J. Han. Spectral regression: A unified approach for sparse subspace learning. In *Seventh IEEE International Conference on Data Mining (ICDM 2007)*, pages 73–82. IEEE, 2007.
- [12] K. Chaudhuri, F. C. Graham, and A. Tsiatas. Spectral clustering of graphs with general degrees in the extended planted partition model. In *COLT*, volume 23, pages 35–1, 2012.
- [13] D. S. Choi. Estimation of monotone treatment effects in network experiments. *arXiv preprint arXiv:1408.4102*, 2014.
- [14] N. A. Christakis and J. H. Fowler. The spread of obesity in a large social network over 32 years. *New England journal of medicine*, 357(4):370–379, 2007.
- [15] F. R. Chung. *Spectral graph theory*, volume 92. American Mathematical Soc., 1997.
- [16] M. B. Cohen, R. Kyng, G. L. Miller, J. W. Pachocki, R. Peng, A. B. Rao, and S. C. Xu. Solving sdd linear systems in nearly $m \log 1/2 n$ time. In *Proceedings of the 46th Annual ACM Symposium on Theory of Computing*, pages 343–352. ACM, 2014.
- [17] D. R. Cox. Regression models and life-tables. *Journal of the Royal Statistical Society. Series B (Methodological)*, pages 187–220, 1972.
- [18] N. Cressie. The origins of kriging. *Mathematical geology*, 22(3):239–252, 1990.
- [19] M. Faverge and P. Ramet. Dynamic scheduling for sparse direct solver on numa architectures. In *PARA ’08*, 2008.
- [20] S. Fortunato. Community detection in graphs. *Physics Reports*, 486(3):75–174, 2010.
- [21] K. Fujimoto and T. W. Valente. Social network influences on adolescent substance use: disentangling structural equivalence from cohesion. *Social Science & Medicine*, 74(12):1952–1960, 2012.

- [22] A. Goldenberg, A. X. Zheng, S. E. Fienberg, and E. M. Airoldi. A survey of statistical network models. *Foundations and Trends® in Machine Learning*, 2(2):129–233, 2010.
- [23] K. M. Harris. *The National Longitudinal Study of Adolescent to Adult Health (Add Health), Waves I & II, 1994-1996; Wave III, 2001-2002; Wave IV, 2007-009 [machine-readable data file and documentation]*. Carolina Population Center, University of North Carolina at Chapel Hill, 2009.
- [24] D. L. Haynie. Delinquent peers revisited: Does network structure matter? *American journal of sociology*, 106(4):1013–1057, 2001.
- [25] C. R. Henderson. Estimation of variance and covariance components. *Biometrics*, 9(2):226–252, 1953.
- [26] S. Kim, W. Pan, and X. Shen. Network-based penalized regression with application to genomic data. *Biometrics*, 69(3):582–593, 2013.
- [27] E. D. Kolaczyk. *Statistical Analysis of Network Data: Methods and Models*. Springer Publishing Company, Incorporated, 1st edition, 2009.
- [28] I. Koutis, G. L. Miller, and R. Peng. Approaching optimality for solving sdd linear systems. In *Foundations of Computer Science (FOCS), 2010 51st Annual IEEE Symposium on*, pages 235–244. IEEE, 2010.
- [29] X. Lacoste, M. Faverge, P. Ramet, S. Thibault, and G. Bosilca. Taking advantage of hybrid systems for sparse direct solvers via task-based runtimes. In *Parallel & Distributed Processing Symposium Workshops (IPDPSW), 2014 IEEE International*, pages 29–38. IEEE, 2014.
- [30] S. R. Land and J. H. Friedman. Variable fusion: A new adaptive signal regression method. Technical report, Technical Report 656, Department of Statistics, Carnegie Mellon University Pittsburgh, 1997.
- [31] C. M. Le, E. Levina, and R. Vershynin. Sparse random graphs: regularization and concentration of the Laplacian. *arXiv preprint arXiv:1502.03049*, 2015.
- [32] L.-f. Lee. Identification and estimation of econometric models with group interactions, contextual factors and fixed effects. *Journal of Econometrics*, 140(2):333–374, 2007.
- [33] C. Li and H. Li. Network-constrained regularization and variable selection for analysis of genomic data. *Bioinformatics*, 24(9):1175–1182, 2008.
- [34] C. Li and H. Li. Variable selection and regression analysis for graph-structured covariates with an application to genomics. *The Annals of Applied Statistics*, 4(3):1498, 2010.
- [35] T. Li, E. Levina, and J. Zhu. *netcoh: Statistical Modeling with Network Cohesion*, 2016. R package version 0.11.
- [36] X. Lin. Identifying peer effects in student academic achievement by spatial autoregressive models with group unobservables. *Journal of Labor Economics*, 28(4):825–860, 2010.
- [37] R. J. Lipton, D. J. Rose, and R. E. Tarjan. Generalized nested dissection. *SIAM journal on numerical analysis*, 16(2):346–358, 1979.

- [38] C. F. Manski. Identification of endogenous social effects: The reflection problem. *The Review of Economic Studies*, 60(3):531–542, 1993.
- [39] C. F. Manski. Identification of treatment response with social interactions. *The Econometrics Journal*, 16(1):S1–S23, 2013.
- [40] L. Michell and P. West. Peer pressure to smoke: the meaning depends on the method. *Health education research*, 11(1):39–49, 1996.
- [41] M. Newman and A. Clauset. Structure and inference in annotated networks. *arXiv preprint arXiv:1507.04001*, 2015.
- [42] W. Pan, B. Xie, and X. Shen. Incorporating predictor network in penalized regression with application to microarray data. *Biometrics*, 66(2):474–484, 2010.
- [43] M. Pearson and L. Michell. Smoke rings: social network analysis of friendship groups, smoking and drug-taking. *Drugs: Education, Prevention, and Policy*, 7(1):21–37, 2000.
- [44] M. Pearson and P. West. Drifting smoke rings. *Connections*, 25(2):59–76, 2003.
- [45] T. Q. Phan and E. M. Airoldi. A natural experiment of social network formation and dynamics. *Proceedings of the National Academy of Sciences*, 112(21):6595–6600, 2015.
- [46] B. Raducanu and F. Dornaika. A supervised non-linear dimensionality reduction approach for manifold learning. *Pattern Recognition*, 45(6):2432–2444, 2012.
- [47] D. G. Rand, S. Arbesman, and N. A. Christakis. Dynamic social networks promote cooperation in experiments with humans. *Proceedings of the National Academy of Sciences*, 108(48):19193–19198, 2011.
- [48] H. Rue and L. Held. *Gaussian Markov random fields: theory and applications*. CRC Press, 2005.
- [49] V. Sadhanala, Y.-X. Wang, and R. J. Tibshirani. Graph sparsification approaches for laplacian smoothing. In *Proceedings of the 19th International Conference on Artificial Intelligence and Statistics*, pages 1250–1259, 2016.
- [50] S. R. Searle, G. Casella, and C. E. McCulloch. *Variance components*, volume 391. John Wiley & Sons, 2009.
- [51] C. R. Shalizi and A. C. Thomas. Homophily and contagion are generically confounded in observational social network studies. *Sociological Methods and Research*, 40(2):211–239, 2011.
- [52] J. Sharpnack, A. Krishnamurthy, and A. Singh. Detecting activations over graphs using spanning tree wavelet bases. *arXiv preprint arXiv:1206.0937*, 2012.
- [53] J. Shi and J. Malik. Normalized cuts and image segmentation. *Pattern Analysis and Machine Intelligence, IEEE Transactions on*, 22(8):888–905, 2000.
- [54] D. A. Spielman. Algorithms, graph theory, and linear equations in laplacian matrices. In *Proceedings of the International Congress of Mathematicians*, volume 4, pages 2698–2722, 2010.
- [55] D. A. Spielman and S.-H. Teng. Spectral sparsification of graphs. *SIAM Journal on Computing*, 40(4):981–1025, 2011.

- [56] J. B. Tenenbaum, V. De Silva, and J. C. Langford. A global geometric framework for nonlinear dimensionality reduction. *science*, 290(5500):2319–2323, 2000.
- [57] R. Tibshirani, M. Saunders, S. Rosset, J. Zhu, and K. Knight. Sparsity and smoothness via the fused lasso. *Journal of the Royal Statistical Society: Series B (Statistical Methodology)*, 67(1):91–108, 2005.
- [58] V. Vapnik. *The nature of statistical learning theory*. Springer Science & Business Media, 2013.
- [59] P. J. Verweij and H. C. Van Houwelingen. Cross-validation in survival analysis. *Statistics in medicine*, 12(24):2305–2314, 1993.
- [60] J. T. Vogelstein, W. G. Roncal, R. J. Vogelstein, and C. E. Priebe. Graph classification using signal-subgraphs: Applications in statistical connectomics. *Pattern Analysis and Machine Intelligence, IEEE Transactions on*, 35(7):1539–1551, 2013.
- [61] E. Vural and C. Guillemot. Out-of-sample generalizations for supervised manifold learning for classification. *IEEE Transactions on Image Processing*, 25(3):1410–1424, 2016.
- [62] G. Wahba et al. Support vector machines, reproducing kernel hilbert spaces and the randomized gacv. *Advances in Kernel Methods-Support Vector Learning*, 6:69–87, 1999.
- [63] L. A. Waller and C. A. Gotway. *Applied spatial statistics for public health data*, volume 368. John Wiley & Sons, 2004.
- [64] Y.-X. Wang, J. Sharpnack, A. Smola, and R. J. Tibshirani. Trend filtering on graphs. *arXiv preprint arXiv:1410.7690*, 2014.
- [65] D. M. Witten and R. Tibshirani. Survival analysis with high-dimensional covariates. *Statistical methods in medical research*, 2009.
- [66] T. Wolf, A. Schroter, D. Damian, and T. Nguyen. Predicting build failures using social network analysis on developer communication. In *Proceedings of the 31st International Conference on Software Engineering*, pages 1–11. IEEE Computer Society, 2009.
- [67] Y. Xu, J. S. Dyer, and A. B. Owen. Empirical stationary correlations for semi-supervised learning on graphs. *The Annals of Applied Statistics*, pages 589–614, 2010.
- [68] W. Yang, C. Sun, and L. Zhang. A multi-manifold discriminant analysis method for image feature extraction. *Pattern Recognition*, 44(8):1649–1657, 2011.
- [69] Y. Zhang, E. Levina, and J. Zhu. Community detection in networks with node features. *arXiv preprint arXiv:1509.01173*, 2015.
- [70] D. Zhou, O. Bousquet, T. N. Lal, J. Weston, and B. Schölkopf. Learning with local and global consistency. In *NIPS*, volume 16, pages 321–328, 2003.
- [71] D. Zhou, J. Huang, and B. Schölkopf. Learning from labeled and unlabeled data on a directed graph. In *Proceedings of the 22nd international conference on Machine learning*, pages 1036–1043. ACM, 2005.

A Proofs

Proof of Proposition 1. The first claim follows directly from the fact that $\mathbf{1}$ is an eigenvector of $P_{X^\perp} + \lambda L$ with eigenvalue 1, since $\mathbf{1} \in \text{col}(X)^\perp$ and $L\mathbf{1} = 0$. To show the second claim, note that the minimum eigenvalue of $P_{X^\perp} + \lambda L$ is the solution of the optimization problem

$$\min_{\|\mathbf{u}\|=1} \mathbf{u}^T (P_{X^\perp} + \lambda L) \mathbf{u}.$$

Assume $\mathbf{u} = \mathbf{u}_1 + \mathbf{u}_2$, where $\mathbf{u}_1 \in \text{col}(X)^\perp$, $\mathbf{u}_2 \in \text{col}(X)$ and $\|\mathbf{u}_1\|^2 + \|\mathbf{u}_2\|^2 = 1$. Then the objective function can be rewritten as

$$\lambda \mathbf{u}^T L \mathbf{u} + \|\mathbf{u}_1\|^2.$$

This is zero if and only if $\|\mathbf{u}_1\| = 0$ and $\mathbf{u}^T L \mathbf{u} = 0$, but these two contradict Assumption 1. As discussed in Section 2.2, the RNC estimator exists whenever $P_{X^\perp} + \lambda L$ is invertible, which shows that the RNC estimate exists.

□

One formula that will be used frequently later is the decomposition of MSE for a vector estimation:

$$\mathbb{E}\|\hat{\boldsymbol{\theta}} - \boldsymbol{\theta}\|^2 = \|\mathbb{E}\hat{\boldsymbol{\theta}} - \boldsymbol{\theta}\|^2 + \text{tr}(\text{Var}(\hat{\boldsymbol{\theta}})),$$

in which we call the second term total variance of $\hat{\boldsymbol{\theta}}$.

We first derive the bias and variance of both the OLS and the RNC estimators. We use $b(\cdot)$ to denote the bias of an estimator. The bias, variance and MSE of the OLS estimator are standard. We state the MSE here for completeness without proof.

Lemma 1. For the OLS estimator given by

$$\hat{\boldsymbol{\beta}}_{OLS} = (X^T X)^{-1} X^T \mathbf{Y}, \quad \hat{\boldsymbol{\alpha}}_{OLS} = \bar{y} \mathbf{1},$$

we have

$$\begin{aligned} \text{MSE}(\hat{\boldsymbol{\alpha}}_{OLS}) &= \|\bar{\boldsymbol{\alpha}} \mathbf{1} - \boldsymbol{\alpha}\|^2 + \frac{\sigma^2}{n}, \\ \text{MSE}(\hat{\boldsymbol{\beta}}_{OLS}) &= \|(X^T X)^{-1} X^T \boldsymbol{\alpha}\|^2 + \sigma^2 \text{tr}((X^T X)^{-1}), \end{aligned}$$

$$\mathbb{E}\|\hat{\mathbf{Y}}_{OLS} - \mathbb{E}\mathbf{Y}\|^2 = \left\| \left(\frac{1}{n} \mathbf{1} \mathbf{1}^T + X(X^T X)^{-1} X^T \right) \boldsymbol{\alpha} - \boldsymbol{\alpha} \right\|^2 + \sigma^2 \left\| \frac{1}{n} \mathbf{1} \mathbf{1}^T + X(X^T X)^{-1} X^T \right\|_F^2.$$

Lemma 2. The bias of the RNC estimator is given by

$$b(\hat{\boldsymbol{\theta}}) = -\lambda(\tilde{X}^T \tilde{X} + \lambda M)^{-1} M \boldsymbol{\theta}. \quad (24)$$

Equivalently, one can write it in the following decomposed form:

$$b(\hat{\boldsymbol{\theta}}) = (b(\hat{\boldsymbol{\alpha}})^T, ((X^T X)^{-1} X^T b(\hat{\boldsymbol{\alpha}}))^T)^T, \quad (25)$$

where $b(\hat{\boldsymbol{\alpha}}) = -(\frac{1}{\lambda} P_{X^\perp} + L)^{-1} L \boldsymbol{\alpha}$, and $P_X = X(X^T X)^{-1} X^T$ is the projection matrix onto $\text{col}(X)$.

The variance of the RNC estimator is given by

$$\text{Var}(\hat{\boldsymbol{\theta}}) = \sigma^2(\tilde{X}^T \tilde{X} + \lambda M)^{-1} \tilde{X}^T \tilde{X} (\tilde{X}^T \tilde{X} + \lambda M)^{-1} \preceq \sigma^2(\tilde{X}^T \tilde{X} + \lambda M)^{-1}.$$

Proof. For the bias term,

$$\begin{aligned} b(\hat{\boldsymbol{\theta}}) &= \mathbb{E}(\tilde{X}^T \tilde{X} + \lambda M)^{-1} \tilde{X}^T Y - \boldsymbol{\theta} \\ &= (\tilde{X}^T \tilde{X} + \lambda M)^{-1} \tilde{X}^T \tilde{X} \boldsymbol{\theta} - \boldsymbol{\theta} \\ &= -\lambda(\tilde{X}^T \tilde{X} + \lambda M)^{-1} M \boldsymbol{\theta}. \end{aligned}$$

Note that we have $M \boldsymbol{\theta} = \begin{bmatrix} L \boldsymbol{\alpha} \\ 0 \end{bmatrix}$. By the block matrix inverse formula, we have

$$(\tilde{X}^T \tilde{X} + \lambda M)^{-1} = \begin{bmatrix} (P_{X^\perp} + \lambda L)^{-1} & (P_{X^\perp} + \lambda L)^{-1} X (X^T X)^{-1} \\ (X^T X)^{-1} X^T (P_{X^\perp} + \lambda L)^{-1} & (X^T X)^{-1} + (X^T X)^{-1} X^T (P_{X^\perp} + \lambda L)^{-1} X (X^T X)^{-1} \end{bmatrix}.$$

Then (25) follows directly from decomposing the bias vector into the $\boldsymbol{\alpha}$ and $\boldsymbol{\beta}$ parts.

The variance can be calculated by the standard OLS formula taking \tilde{X} as the design matrix. The positive semi-definiteness follows from the fact that

$$X^T X \preceq X^T X + \lambda M$$

whenever M is positive semi-definite. □

From Lemma 2 and the bias-variance decomposition, we can directly get the closed form expressions for the MSE of RNC estimation. In particular,

$$\begin{aligned} \text{MSE}(\boldsymbol{\theta}) &= \|\lambda(P_{X^\perp} + \lambda L)^{-1} L \boldsymbol{\alpha}\|^2 + \|\lambda(X^T X)^{-1} X^T (P_{X^\perp} + \lambda L)^{-1} L \boldsymbol{\alpha}\|^2 \\ &\quad + \sigma^2 \text{tr}((\tilde{X}^T \tilde{X} + \lambda M)^{-1} \tilde{X}^T \tilde{X} (\tilde{X}^T \tilde{X} + \lambda M)^{-1}). \end{aligned} \quad (26)$$

Proof of Theorem 1. Note that $P_{X^\perp} + \lambda L \succeq \nu I$. Thus the squared bias term for $\boldsymbol{\alpha}$ is

$$\|\lambda(P_{X^\perp} + \lambda L)^{-1} L \boldsymbol{\alpha}\|^2 \leq \frac{\lambda^2}{\nu^2} \|L \boldsymbol{\alpha}\|^2.$$

The total variance of $\hat{\boldsymbol{\alpha}}$ can be upper bounded by

$$\text{tr}(\sigma^2(P_{X^\perp} + \lambda L)^{-1}) \leq \frac{\sigma^2}{\nu} \text{tr}(I) = \frac{n\sigma^2}{\nu}.$$

Thus the bound (12) on $\text{MSE}(\hat{\boldsymbol{\alpha}})$ follows.

From Lemma 2, we have

$$\begin{aligned}
\|b(\hat{\beta})\|^2 &= b(\hat{\alpha})^T X (X^T X)^{-1} (X^T X)^{-1} X^T b(\hat{\alpha}) \\
&\leq \frac{1}{\mu} b(\hat{\alpha})^T X (X^T X)^{-1} (X^T X) (X^T X)^{-1} X^T b(\hat{\alpha}) \\
&= \frac{1}{\mu} b(\hat{\alpha})^T X (X^T X)^{-1} X^T b(\hat{\alpha}) = \frac{1}{\mu} b(\hat{\alpha})^T (P_X b(\hat{\alpha})) \\
&= \frac{1}{\mu} \|P_X b(\hat{\alpha})\|^2 \leq \frac{1}{\mu} \|b(\hat{\alpha})\|^2 \leq \frac{\lambda^2}{\nu^2 \mu} \|L\alpha\|^2.
\end{aligned} \tag{27}$$

By Lemma 2 and Schur complement, the covariance matrix of $\hat{\beta}$ is

$$\begin{aligned}
\text{Var}(\hat{\beta}) &\preceq \sigma^2 (X^T X)^{-1} + \sigma^2 (X^T X)^{-1} X^T (P_{X^\perp} + \lambda L)^{-1} X (X^T X)^{-1} \\
&\preceq \sigma^2 (X^T X)^{-1} + \frac{\sigma^2}{\nu} (X^T X)^{-1} X^T X (X^T X)^{-1} = \sigma^2 \left(\frac{1}{\nu} + 1 \right) (X^T X)^{-1}.
\end{aligned} \tag{28}$$

Combining the squared bias (27) and variance (28) gives the bound (13) on $\text{MSE}(\hat{\beta})$. The mean squared prediction error can be similarly derived. With $\hat{V} = \tilde{X}\hat{\theta}$, we have

$$b(\hat{V}) = \tilde{X}b(\hat{\theta}) = -\lambda\tilde{X}(\tilde{X}^T\tilde{X} + \lambda M)^{-1}M\theta,$$

and

$$\text{Var}(\hat{V}) = \sigma^2 \tilde{X}(\tilde{X}^T\tilde{X} + \lambda M)^{-1}\tilde{X}^T\tilde{X}(\tilde{X}^T\tilde{X} + \lambda M)^{-1}\tilde{X}^T.$$

Thus

$$\begin{aligned}
\mathbb{E}\|\hat{V} - \mathbb{E}Y\|^2 &= \|b(\hat{V})\|^2 + \text{tr}(\text{Var}(\hat{V})) \\
&\leq \lambda^2 (L\alpha)^T (P_{X^\perp} + \lambda L)^{-1} (L\alpha) + \sigma^2 \text{tr}(S_\lambda^T S_\lambda) \\
&\leq \frac{\lambda^2}{\nu} \|L\alpha\|^2 + \sigma^2 \|S_\lambda\|_F^2.
\end{aligned}$$

This completes the proof of Theorem 1. \square

Proof of Proposition 2. Let τ_i be the i th largest eigenvalue of L with the associated eigenvector \mathbf{u}_k . Assume $\alpha = \sum_{i=n-k+1}^n \rho_i \mathbf{u}_i$. Without loss of generality, assume $\|\alpha\|^2 = n$ thus $\sum_{i=n-k+1}^n \rho_i^2 = n$. In this situation, we need

$$\|L\alpha\|^2 = \sum_{i=n-k+1}^n \rho_i^2 \tau_i^2 \leq n^c.$$

Since $\sum_{i=n-k+1}^n \rho_i^2 \tau_i^2 \leq \tau_{n-k+1}^2 \sum_{i=n-k+1}^n \rho_i^2 = n \tau_{n-k+1}^2$, it is sufficient to have $\rho_{n-k+1}^2 \leq n^{-(1-c)}$. By basic graph spectral theory, we can see that all of the eigenvalues of the lattice network can be written as

$$2 \sin^2\left(\frac{\pi}{2} \frac{i}{\sqrt{n}}\right) + 2 \sin^2\left(\frac{\pi}{2} \frac{j}{\sqrt{n}}\right)$$

for some $(i, j) \in [\sqrt{n}] \times [\sqrt{n}]$. Thus it is sufficient to ensure

$$2 \sin^2\left(\frac{\pi}{2} \frac{i}{\sqrt{n}}\right) + 2 \sin^2\left(\frac{\pi}{2} \frac{j}{\sqrt{n}}\right) \leq 2\left(\frac{\pi}{2}\right) \frac{i^2}{n} + 2\left(\frac{\pi}{2}\right) \frac{j^2}{n} \leq n^{-\frac{1-c}{2}}.$$

For reasonably large n , the proportion of pairs (i, j) satisfying the condition in $[\sqrt{n}] \times [\sqrt{n}]$ is approximately the area ratio between a $1/4$ sphere and a square, which is $\frac{1}{2\pi} \frac{n^{\frac{1+c}{2}}}{n}$. Therefore, the number of eigenvalues that satisfies the requirement is at least $Cn^{\frac{1+c}{2}}$ for some constant C .

□

For the easiness of comparison, we also give similar error bounds for the linear null model estimate, which is obtained as

$$\tilde{\boldsymbol{\theta}} = (\tilde{\boldsymbol{\alpha}}, \tilde{\boldsymbol{\beta}}) = \operatorname{argmin}_{\boldsymbol{\alpha}, \boldsymbol{\beta}} \|\mathbf{Y} - \mathbf{X}\boldsymbol{\beta} - \boldsymbol{\alpha}\|^2 + \lambda \|\boldsymbol{\alpha}\|^2 \quad (29)$$

The following proposition shows that in the case of linear regression, the null model gives the same estimate of $\boldsymbol{\beta}$ as OLS.

Lemma 3. Let $\tilde{\boldsymbol{\beta}}$ be the estimate from null model. Then we have

$$\tilde{\boldsymbol{\beta}} = \hat{\boldsymbol{\beta}}_{OLS} = (\mathbf{X}^T \mathbf{X})^{-1} \mathbf{X}^T \mathbf{Y}.$$

As a result, we have $\tilde{\boldsymbol{\alpha}} = \frac{1}{1+\lambda} (\mathbf{Y} - \mathbf{X}\hat{\boldsymbol{\beta}}_{OLS})$. Moreover, the estimation errors for the null model satisfy

$$\begin{aligned} \text{MSE}(\tilde{\boldsymbol{\alpha}}) &= \|\boldsymbol{\alpha} - \frac{1}{1+\lambda} P_{X^\perp} \boldsymbol{\alpha}\|^2 + \frac{(n-p)\sigma^2}{(1+\lambda)^2} \\ &\leq \frac{\lambda^2}{(1+\lambda)^2} \|\boldsymbol{\alpha}\|^2 + \frac{1}{(1+\lambda)^2} \|P_{X^\perp} \boldsymbol{\alpha}\|^2 + \frac{(n-p)\sigma^2}{(1+\lambda)^2}, \\ \text{MSE}(\tilde{\boldsymbol{\beta}}) &= \|(X^T X)^{-1} X^T \boldsymbol{\alpha}\|^2 + \sigma^2 \operatorname{tr}((X^T X)^{-1}), \\ \mathbb{E}\|\tilde{\mathbf{Y}} - \mathbb{E}\mathbf{Y}\|^2 &= \frac{\lambda^2}{(1+\lambda)^2} \|P_{X^\perp} \boldsymbol{\alpha}\|^2 + \sigma^2 \left(p + \frac{n-p}{(1+\lambda)^2}\right). \end{aligned}$$

In particular, the optimal MSPE is

$$\mathbb{E}\|\tilde{\mathbf{Y}} - \mathbb{E}\mathbf{Y}\|^2 = \frac{(n-p)\sigma^2 \|P_{X^\perp} \boldsymbol{\alpha}\|^2}{(n-p)\sigma^2 + \|P_{X^\perp} \boldsymbol{\alpha}\|^2}$$

which is achieved when $\lambda = \frac{(n-p)\sigma^2}{\|P_{X^\perp} \boldsymbol{\alpha}\|^2}$.

Proof of Lemma 3. Notice that \mathbf{X} is column centered, so we always have $\mathbf{1}^T \mathbf{X} = 0$, which ensures

$$\hat{\boldsymbol{\beta}}_{OLS} = (\mathbf{X}^T \mathbf{X})^{-1} \mathbf{X}^T \mathbf{Y}.$$

The solution of the null model is given by

$$\begin{bmatrix} \tilde{\boldsymbol{\alpha}} \\ \tilde{\boldsymbol{\beta}} \end{bmatrix} = \begin{bmatrix} (1+\lambda)I_n & \mathbf{X} \\ \mathbf{X}^T & \mathbf{X}^T \mathbf{X} \end{bmatrix}^{-1} \begin{bmatrix} \mathbf{Y} \\ \mathbf{X}^T \mathbf{Y} \end{bmatrix}. \quad (30)$$

By block matrix inverse formula, we have

$$\begin{aligned}\tilde{\boldsymbol{\beta}} &= -\frac{1+\lambda}{\lambda} \frac{1}{1+\lambda} (X^T X)^{-1} X^T Y + \frac{1+\lambda}{\lambda} (X^T X)^{-1} X^T Y \\ &= (X^T X)^{-1} X^T Y = \hat{\boldsymbol{\beta}}_{OLS}.\end{aligned}$$

The formula for $\tilde{\boldsymbol{\alpha}}$ and all the error bounds can then be obtained similarly as in Theorem 1. \square

Proof of Theorem 3. Denote $\ell(\boldsymbol{\alpha} + X\boldsymbol{\beta}; \mathbf{Y})$ by $\ell(\boldsymbol{\theta})$. Define

$$M = \begin{bmatrix} L & 0_{n \times p} \\ 0_{p \times n} & 0_{p \times p} \end{bmatrix}.$$

The matrix M^* is defined similarly. Then by the optimality of $\hat{\boldsymbol{\theta}}^*$ under f^* , we have

$$\begin{aligned}\ell(\hat{\boldsymbol{\theta}}^*) + \lambda \hat{\boldsymbol{\theta}}^{*T} M^* \hat{\boldsymbol{\theta}}^* &= f^*(\hat{\boldsymbol{\theta}}^*) \\ &\leq f^*(\hat{\boldsymbol{\theta}}) \\ &= \ell(\hat{\boldsymbol{\theta}}) + \lambda \hat{\boldsymbol{\theta}}^{T} M^* \hat{\boldsymbol{\theta}} \\ &\leq \ell(\hat{\boldsymbol{\theta}}) + \lambda(1 + \epsilon) \hat{\boldsymbol{\theta}}^{T} M \hat{\boldsymbol{\theta}},\end{aligned}\tag{31}$$

in which the last inequality can be easily derived from (17) by noticing that M^* has all zeros except in the upper left corner. By Taylor expansion of ℓ at $\hat{\boldsymbol{\theta}}$, we have

$$\begin{aligned}\ell(\hat{\boldsymbol{\theta}}^*) &= \ell(\hat{\boldsymbol{\theta}}) + \nabla \ell(\hat{\boldsymbol{\theta}})^T (\hat{\boldsymbol{\theta}}^* - \hat{\boldsymbol{\theta}}) + \frac{1}{2} (\hat{\boldsymbol{\theta}}^* - \hat{\boldsymbol{\theta}})^T \nabla^2 \ell(\bar{\boldsymbol{\theta}}) (\hat{\boldsymbol{\theta}}^* - \hat{\boldsymbol{\theta}}) \\ &= \ell(\hat{\boldsymbol{\theta}}) + \nabla \ell(\hat{\boldsymbol{\theta}})^T (\hat{\boldsymbol{\theta}}^* - \hat{\boldsymbol{\theta}}) + \frac{1}{2} (\hat{\boldsymbol{\theta}}^* - \hat{\boldsymbol{\theta}})^T (\nabla^2 \ell(\bar{\boldsymbol{\theta}}) + 2\lambda M) (\hat{\boldsymbol{\theta}}^* - \hat{\boldsymbol{\theta}}) - \lambda (\hat{\boldsymbol{\theta}}^* - \hat{\boldsymbol{\theta}})^T M (\hat{\boldsymbol{\theta}}^* - \hat{\boldsymbol{\theta}}) \\ &\geq \ell(\hat{\boldsymbol{\theta}}) + \nabla \ell(\hat{\boldsymbol{\theta}})^T (\hat{\boldsymbol{\theta}}^* - \hat{\boldsymbol{\theta}}) + \frac{m}{2} \|\hat{\boldsymbol{\theta}}^* - \hat{\boldsymbol{\theta}}\|^2 - \lambda (\hat{\boldsymbol{\theta}}^* - \hat{\boldsymbol{\theta}})^T M (\hat{\boldsymbol{\theta}}^* - \hat{\boldsymbol{\theta}}).\end{aligned}\tag{32}$$

In (32), $\bar{\boldsymbol{\theta}}$ is some point between $\hat{\boldsymbol{\theta}}$ and $\hat{\boldsymbol{\theta}}^*$ and the last inequality comes from the strong convexity assumption on f . Substituting (32) into (31) yields

$$\begin{aligned}\frac{m}{2} \|\hat{\boldsymbol{\theta}}^* - \hat{\boldsymbol{\theta}}\|^2 &\leq -\nabla \ell(\hat{\boldsymbol{\theta}})^T (\hat{\boldsymbol{\theta}}^* - \hat{\boldsymbol{\theta}}) + \lambda (\hat{\boldsymbol{\theta}}^* - \hat{\boldsymbol{\theta}})^T M (\hat{\boldsymbol{\theta}}^* - \hat{\boldsymbol{\theta}}) + \lambda(1 + \epsilon) \hat{\boldsymbol{\theta}}^{T} M \hat{\boldsymbol{\theta}} - \lambda \hat{\boldsymbol{\theta}}^{*T} M^* \hat{\boldsymbol{\theta}}^* \\ &= -\nabla \ell(\hat{\boldsymbol{\theta}})^T (\hat{\boldsymbol{\theta}}^* - \hat{\boldsymbol{\theta}}) + \lambda(2 + \epsilon) \hat{\boldsymbol{\theta}}^{T} M \hat{\boldsymbol{\theta}} + \lambda \hat{\boldsymbol{\theta}}^{*T} M \hat{\boldsymbol{\theta}}^* - \lambda \hat{\boldsymbol{\theta}}^{*T} M^* \hat{\boldsymbol{\theta}}^* - 2\lambda \hat{\boldsymbol{\theta}}^{T} M \hat{\boldsymbol{\theta}}^*.\end{aligned}\tag{33}$$

Since $\hat{\boldsymbol{\theta}}$ is the minimizer of f , we have the stationary condition

$$\nabla \ell(\hat{\boldsymbol{\theta}}) + 2\lambda M \hat{\boldsymbol{\theta}} = \mathbf{0}.\tag{34}$$

Substituting (34) into (33) gives

$$\begin{aligned}
\frac{m}{2} \|\hat{\boldsymbol{\theta}}^* - \hat{\boldsymbol{\theta}}\|^2 &\leq 2\lambda\hat{\boldsymbol{\theta}}^T M(\hat{\boldsymbol{\theta}}^* - \hat{\boldsymbol{\theta}}) + \lambda(2 + \epsilon)\hat{\boldsymbol{\theta}}^T M\hat{\boldsymbol{\theta}} + \lambda\hat{\boldsymbol{\theta}}^{*T} M\hat{\boldsymbol{\theta}}^* - \lambda\hat{\boldsymbol{\theta}}^{*T} M^*\hat{\boldsymbol{\theta}}^* - 2\lambda\hat{\boldsymbol{\theta}}^T M\hat{\boldsymbol{\theta}}^* \\
&= \epsilon\lambda\hat{\boldsymbol{\theta}}^T M\hat{\boldsymbol{\theta}} + \lambda\hat{\boldsymbol{\theta}}^{*T} M\hat{\boldsymbol{\theta}}^* - \lambda\hat{\boldsymbol{\theta}}^{*T} M^*\hat{\boldsymbol{\theta}}^* \\
&\leq \epsilon\lambda\hat{\boldsymbol{\theta}}^T M\hat{\boldsymbol{\theta}} + \epsilon\lambda\hat{\boldsymbol{\theta}}^{*T} M\hat{\boldsymbol{\theta}}^* \\
&\leq \epsilon\lambda\hat{\boldsymbol{\theta}}^T M\hat{\boldsymbol{\theta}} + \frac{\epsilon}{1-\epsilon}\lambda\hat{\boldsymbol{\theta}}^{*T} M\hat{\boldsymbol{\theta}}^* \\
&= \epsilon\lambda\hat{\boldsymbol{\alpha}}^T L\hat{\boldsymbol{\alpha}} + \frac{\epsilon}{1-\epsilon}\lambda\hat{\boldsymbol{\alpha}}^{*T} L\hat{\boldsymbol{\alpha}}^*, \tag{35}
\end{aligned}$$

where we use (17) again. This gives the bound we need. However, it would be better to have a bound with a dominant term that only depends on $\hat{\boldsymbol{\alpha}}$ and L . Thus we rearrange the terms as

$$\begin{aligned}
\frac{m}{2} \|\hat{\boldsymbol{\theta}}^* - \hat{\boldsymbol{\theta}}\|^2 &\leq \epsilon\lambda\hat{\boldsymbol{\alpha}}^T L\hat{\boldsymbol{\alpha}} + \frac{\epsilon}{1-\epsilon}\lambda\hat{\boldsymbol{\alpha}}^{*T} L\hat{\boldsymbol{\alpha}}^* \\
&\leq \epsilon\lambda\hat{\boldsymbol{\alpha}}^T L\hat{\boldsymbol{\alpha}} + (1 + 2\epsilon)\lambda\hat{\boldsymbol{\alpha}}^{*T} L\hat{\boldsymbol{\alpha}}^* \\
&= \epsilon\lambda[2\hat{\boldsymbol{\alpha}}^T L\hat{\boldsymbol{\alpha}} + (\hat{\boldsymbol{\alpha}}^{*T} L\hat{\boldsymbol{\alpha}}^* - \hat{\boldsymbol{\alpha}}^T L\hat{\boldsymbol{\alpha}}) + 2\epsilon\hat{\boldsymbol{\alpha}}^{*T} L\hat{\boldsymbol{\alpha}}^*] \\
&\leq \epsilon\lambda[2\hat{\boldsymbol{\alpha}}^T L\hat{\boldsymbol{\alpha}} + |\hat{\boldsymbol{\alpha}}^{*T} L\hat{\boldsymbol{\alpha}}^* - \hat{\boldsymbol{\alpha}}^T L\hat{\boldsymbol{\alpha}}| + 2\epsilon\hat{\boldsymbol{\alpha}}^{*T} L\hat{\boldsymbol{\alpha}}^*], \tag{36}
\end{aligned}$$

in which the second inequality comes from the fact that $\frac{1}{1-\epsilon} < 1 + 2\epsilon$ for $\epsilon < 1/2$. Note that we expect $|\hat{\boldsymbol{\alpha}}^{*T} L\hat{\boldsymbol{\alpha}}^* - \hat{\boldsymbol{\alpha}}^T L\hat{\boldsymbol{\alpha}}|$ to be negligible compared to the first term.

We now proceed to proving the second bound that only involves $\|\hat{\boldsymbol{\alpha}}\|$. By Taylor expansion, we have, for any $\boldsymbol{\theta}, \boldsymbol{\theta}_0 \in \mathbb{R}^n$,

$$\begin{aligned}
f^*(\boldsymbol{\theta}) &= f^*(\boldsymbol{\theta}_0) + \nabla f^*(\boldsymbol{\theta}_0)^T(\boldsymbol{\theta} - \boldsymbol{\theta}_0) + \frac{1}{2}(\boldsymbol{\theta} - \boldsymbol{\theta}_0)^T \nabla^2 f^*(\tilde{\boldsymbol{\theta}})(\boldsymbol{\theta} - \boldsymbol{\theta}_0) \\
&\geq f^*(\boldsymbol{\theta}_0) + \nabla f^*(\boldsymbol{\theta}_0)^T(\boldsymbol{\theta} - \boldsymbol{\theta}_0) + \frac{m}{2}\|\boldsymbol{\theta} - \boldsymbol{\theta}_0\|^2,
\end{aligned}$$

where the inequality follows from strong convexity. In particular, taking $\boldsymbol{\theta} = \hat{\boldsymbol{\theta}}$ and $\boldsymbol{\theta}_0 = \hat{\boldsymbol{\theta}}^*$ and noticing that $\nabla f^*(\hat{\boldsymbol{\theta}}^*) = \mathbf{0}$, we get

$$\|\hat{\boldsymbol{\theta}}^* - \hat{\boldsymbol{\theta}}\|^2 \leq \frac{2}{m}(f^*(\hat{\boldsymbol{\theta}}) - f^*(\hat{\boldsymbol{\theta}}^*)).$$

Strong convexity also implies (equation (9.9) of [9]) that

$$(f^*(\hat{\boldsymbol{\theta}}) - f^*(\hat{\boldsymbol{\theta}}^*)) \leq \frac{1}{2m}\|\nabla f^*(\hat{\boldsymbol{\theta}})\|^2.$$

Combining the two parts, we have

$$\|\hat{\boldsymbol{\theta}}^* - \hat{\boldsymbol{\theta}}\|^2 \leq \frac{1}{m^2}\|\nabla f^*(\hat{\boldsymbol{\theta}})\|^2 = \frac{1}{m^2}\|\nabla f^*(\hat{\boldsymbol{\theta}}) - \nabla f(\hat{\boldsymbol{\theta}})\|^2, \tag{37}$$

in which the last equality comes from the fact that $\nabla f(\hat{\boldsymbol{\theta}}) = \mathbf{0}$. From (18), the gradients of f and f^* are

$$\nabla f(\hat{\boldsymbol{\theta}}) = \nabla \ell + 2\lambda M\hat{\boldsymbol{\theta}}, \quad \nabla f^*(\hat{\boldsymbol{\theta}}) = \nabla \ell + 2\lambda M^*\hat{\boldsymbol{\theta}}.$$

Thus the difference between $\hat{\boldsymbol{\theta}}^*$ and $\hat{\boldsymbol{\theta}}$ can be bounded by

$$\|\hat{\boldsymbol{\theta}}^* - \hat{\boldsymbol{\theta}}\|^2 \leq \frac{1}{m^2} \|2\lambda(M - M^*)\hat{\boldsymbol{\theta}}\|^2. \quad (38)$$

Finally, from (17), we obtain

$$\begin{aligned} \|2\lambda(M - M^*)\hat{\boldsymbol{\theta}}\|^2 &= \|2\lambda(L - L^*)\hat{\boldsymbol{\alpha}}\|^2 \\ &\leq 4\lambda^2 \|L - L^*\|_2^2 \|\hat{\boldsymbol{\alpha}}\|^2 \\ &\leq 4\lambda^2 \epsilon^2 \|L\|_2^2 \|\hat{\boldsymbol{\alpha}}\|^2. \end{aligned} \quad (39)$$

Combining (38) and (39) yields the second bound and completes the proof. \square

B Complexity of solving RNC estimator by block elimination

We calculate the complexity of solving RNC estimator here assuming the block elimination strategy described in Section 2.7 is used. The first major part is solving an $n \times n$ sparse symmetric diagonal dominant system to obtain $(I + \lambda L)^{-1}X$ and $(I + \lambda L)^{-1}\mathbf{b}_1$ in the estimator. Using the linear system notations, we want to solve

$$A\mathbf{x} = \mathbf{b}$$

where $A = I + \lambda L$. Naively solve it by Cholesky decomposition ignoring special structures would result in $O(n^3)$ operations. When A is sparse as in a great many of applications, we can first find a permutation matrix P to permute A and then find sparse factorization for the resulting permuted matrix

$$PAP^T = LL^T.$$

The operation counts in this step depends on the heuristic algorithm to find a good permutation, the number of nonzero elements in A (which is $n + 2|E|$ in our setting) and the positions of these nonzeros (depicted by the network). Roughly speaking, it depends on $\sum_i d_i^2$ [54]. Though the general complexity is not available, it is shown in [37] that the complexity for the network transformed from a $\sqrt{n} \times \sqrt{n}$ grid is $O(n^{3/2})$ by using an algorithm called George's Nested Dissection. Solving both $(I + \lambda L)^{-1}X$ and $(I + \lambda L)^{-1}\mathbf{b}_1$ thus requires $O(n^{3/2} + pn)$ and when n dominates p , we just have $O(n^{3/2})$ there. We refer readers to [37] for details.

Alternatively, one can solve the system approximately by iterative methods [54, 28]. In particular, [28] propose an iterative algorithm with preconditioning such that for any n -node network, an approximate solution $\hat{\mathbf{x}}$ of accuracy

$$\|\hat{\mathbf{x}} - A^{-1}\mathbf{b}\|_A < \epsilon \|A^{-1}\mathbf{b}\|_A$$

can be computed in expected time $O(m \log^2 n \log(1/\epsilon))$ where $m = n + 2|E|$ and the A -norm is defined by

$$\|\mathbf{x}\|_A = \sqrt{\mathbf{x}^T A \mathbf{x}}.$$

To solve both $(I + \lambda L)^{-1}X$ and $(I + \lambda L)^{-1}\mathbf{b}_1$, this is expected to takes $O(pm \log^2 n \log(1/\epsilon))$ operations. Notice that even if A is fully dense with n^2 nonzero entries, the cost is still much lower than the naive solving.

The rest steps in the block elimination only involve matrix multiplications and general

solving for a $p \times p$ symmetric positive definite system. The order is then $O(np^2 + p^3)$, the same as OLS procedure.

In summary, if one tries to compute the estimator exactly, the order depends on the network connecting the samples. When the network is from a $\sqrt{n} \times \sqrt{n}$ grid, the complexity is in the order of $O(n^{3/2} + pn + np^2 + p^3)$. If approximate methods are used instead, the order is expected to be $O(p(n + 2|E|) \log^3 n + np^2 + p^3)$ for general networks with high accuracy (taking approximation tolerance $\epsilon = O(1/n)$).

Both of dense and sparse Cholesky factorizations can be further parallelized on modern distributed systems [8, 19, 29], when high computational performance is needed. The complexity in such settings heavily depends the systems.